J Geod (2006) 80: 353–372
DOI 10.1007/s00190-006-0072-6

ORIGINAL ARTICLE

G. Beutler · A. Jäggi · U. Hugentobler · L. Mervart

Efficient satellite orbit modelling using pseudo-stochastic parameters

Received: 15 September 2005 / Accepted: 15 June 2006 / Published online: 24 August 2006

Abstract If the force field acting on an artificial Earth satellite is not known a priori with sufficient accuracy to represent its observations on their accuracy level, one may introduce so-called pseudo-stochastic parameters into an orbit determination process, e.g. instantaneous velocity changes at user-defined epochs or piecewise constant accelerations in user-defined adjacent time subintervals or piecewise linear and continuous accelerations in adjacent time subintervals. The procedures, based on standard least-squares, associated with such parameterizations are well established, but they become inefficient (slow) if the number of pseudo-stochastic parameters becomes large. We develop two efficient methods to solve the orbit determination problem in the presence of pseudo-stochastic parameters. The results of the methods are identical to those obtained with conventional least-squares algorithms. The first efficient algorithm also provides the full variance–covariance matrix; the second, even more efficient algorithm, only parts of it.

Keywords Orbit modelling · Efficient orbit determination · Pseudo-stochastic parameters

1 Introduction

In satellite geodesy, one often has to cope with the problem that the force field acting on a satellite is not known with sufficient accuracy when invoking an orbit determination procedure. A problem of this type is, e.g. encountered when analysing the orbits of GPS satellites. It is virtually impossible to predict the effect of solar (and possibly albedo) radiation pressure on the satellite orbits with sufficient accuracy to model the GPS observations (the so-called pseudoranges, based on the GPS code or the carrier-phase observable) to an appropriate accuracy level (mm for the GPS phase observable). Another even more demanding problem is encountered when modelling the orbits of low-Earth orbiting satellites (LEOs) equipped with spaceborne GPS receivers. In addition to radiation pressure, atmospheric drag and possibly an insufficient knowledge of the Earth's gravity field aggravate the problem.

The problem of an insufficiently known force field may be dealt with in several ways:

1. One may replace the deterministic equations of motion by stochastic differential equations. This approach replaces the classical least-squares parameter estimation theory by Kalman or Bayesian filter techniques (Strang and Borre 1997).
2. One may represent the unknown forces by Fourier series using the revolution period of the satellites as fundamental period (Colombo 1989). The coefficients of the Fourier series are parameters of the orbit determination process.
3. One may introduce empirical parameters into a classical least-squares (LSQ) orbit determination scheme. This was, e.g. proposed by Beutler et al. (1994), where so-called pseudo-stochastic pulses, instantaneous velocity changes in pre-defined directions and at pre-defined epochs, are introduced, or by Visser and van den IJssel (2003), where piecewise constant accelerations, also called empirical accelerations, are proposed.

The advantage of the first approach resides in the fact that each orbit is modelled in the entire time interval considered by a constant, small number of active parameters. The disadvantage is that rather laborious matrix operations have to be performed at each observation epoch (which is why often only a small sample of all observations, e.g. one observation epoch per 5 min, is actually processed).

G. Beutler (✉) · A. Jäggi · U. Hugentobler
Astronomical Institute, University of Bern, Sidlerstrasse 5,
Bern 3012, Switzerland
E-mail: gerhard.beutler@aiub.unibe.ch
E-mail: adrian.jaeggi@aiub.unibe.ch
E-mail: urs.hugentobler@aiub.unibe.ch
Tel.: +41-31-6318591
Fax: +41-31-6313869

L. Mervart
Institute of Advanced Geodesy, Czech Technical University, K-152,
FSvCVVT, Thakurova 7, Prague 6-Dejvice 16629, Czech Republic
E-mail: leos.mervart@aiub.unibe.ch
Tel.: +420-2-24354806
Fax: +420-2-24354343

The second approach exploits the orbital characteristics. Many, if not most, of the unknown forces have once-per-revolution characteristics. It is therefore usually possible to obtain a good orbit representation with a modest number of parameters (truncating the Fourier series after low-order terms). The method is, on the other hand, not well suited when trying to absorb effects due to momentum dumps or a slightly wrong attitude, which are not (or only marginally) correlated with the satellite's revolution period. In addition, and this is an important argument from the point of view of efficiency, one has to set up and solve one variational equation (see Sect. 2) for each of the parameters. This option of coping with unknown forces is also described in Beutler et al. (1994). It is used by the Center for Orbit Determination in Europe (CODE) (together with the third method) with a decomposition, which is particularly well suited for absorbing the effects due to radiation pressure (Hugentobler et al. 2003).

The third approach is attractive if many parameters have to be solved for (of the order of hundred or more per revolution). The method is thus particularly well suited for LEO orbit determination. If pseudo-stochastic parameters are used, the partial derivatives associated with them may all be represented as linear combinations of a small set of numerically integrated partial derivatives (Jäggi et al. 2006). The problem of this approach is, however, its inefficiency if the number of parameters (and therefore the dimension of the resulting normal equation system) becomes large (comparable to three times the number of observation epochs).

In this article, we uniquely deal with the third approach and we use LEO orbits as examples. More specifically, we address the problem of efficiency when introducing pseudo-stochastic parameters. Such parameters are introduced to reduce the effect of an insufficiently known force field. It is intuitively clear that these effects may (and in general will) be absorbed by frequently introduced velocity changes or by piecewise constant accelerations. The success of the procedure may be judged by the RMS a posteriori of the original observations, which should be of the same order as the (hopefully known) a priori RMS.

Let us point out, however, that a small RMS error a posteriori does not necessarily mean that the resulting orbits are of better quality. The danger of over-parameterization always exists (although it may be attenuated by applying appropriate constraints on the parameters). Let us also point out that our methods allow it in principle to study the correlation between the pseudo-stochastic parameters and the "normal" orbit parameters, provided that we decide to generate the full variance–covariance matrix (see the subsequent discussion). Our approach will be explained in detail for the case of pseudo-stochastic pulses and only outlined for piecewise constant accelerations (the corresponding modifications are minor in nature). For results achieved with different parameterizations, we refer to Jäggi et al. (2006).

In Sect. 2, we introduce the notation and briefly review equations of motion, associated variational equations, the observation equations, and the normal equation system associated with the simplest orbit determination problem, where only six orbit parameters (corresponding to the initial position and velocity vector) are set up. In Sect. 3, we will introduce pseudo-stochastic pulses in addition to the six parameters mentioned above. In Sect. 4, we will discuss the structure of the resulting normal equation system in detail and show how it may be set up efficiently. Its solution will, by definition, not only provide the solution consisting of the six initial osculating elements and all pseudo-stochastic pulses, but also the full variance–covariance matrix associated with the entire parameter set.

In Sect. 5, we develop an even more efficient method, where the number of active parameters is always "small" (i.e. when setting up and solving the parameter estimation problem). The resulting method is closely related to a Bayesian filter, but may be used in a much more general environment. The only drawback of the method is that the full variance–covariance matrix is not available. However, the variance–covariance matrix associated with the initial osculating elements is available, as well as the variance–covariance matrices associated with each set of pseudo-stochastic pulses referring to one and the same epoch.

In both Sects. 4 and 5, we generalize the problem to a parameter estimation environment, where not only deterministic and pseudo-stochastic orbit parameters, but also other parameters (e.g. ambiguity parameters) have to be considered. Whether or not the resulting parameter estimation procedures are (still) efficient depends almost uniquely on the number of simultaneously active parameters.

In Sects. 6–8, we develop the methods related to piecewise constant accelerations, where we proceed in analogy to the case of pulses: in Sect. 6, we introduce the equations of motion and the observation equations related to the case of piecewise constant accelerations. In Sect. 7, we analyze the structure of the full normal equation system. We show that the full system is closely related to the corresponding system associated with pseudo-stochastic pulses. There are important differences, which do, however, still allow for an efficient setup of the normal equation system. In Sect. 8, we develop a filter-type approach that avoids the setup of the full normal equation system. Sect. 9 briefly addresses the case of piecewise linear accelerations.

In Sect. 10, the implementation of the methods into the Bernese GPS software (Hugentobler et al. 2005) is outlined and the algorithms are applied to several LEO orbit determination problems. The efficiency of the three types of solutions (conventional, efficient solution using the structure of the full normal equation system, filter-like approach) and of different parameterizations is studied.

2 Equations of motion, variational equations and observations

Let us assume that the trajectory $\mathbf{r}(t)$ of a satellite may be described approximately by the following deterministic ordinary differential equation system; the satellite's equation of motion:

$$\ddot{\mathbf{r}} = \mathbf{f}\,(\mathbf{r}, \dot{\mathbf{r}}, t)\,, \tag{1}$$

where $\dot{\mathbf{r}}$ is the first and $\ddot{\mathbf{r}}$ the second time-derivative of the geocentric position vector of the satellite's center of mass and $\mathbf{f}\,(\mathbf{r}, \dot{\mathbf{r}}, t)$ is the force per mass unit acting on the satellite. Gravitational and surface forces (drag and radiation pressure) may be contained in the latter term.

Let us now consider a particular solution $\mathbf{r}_0(t)$ of Eq. 1, which is characterized by the initial osculating elements E_i^0, $i = 1, 2, \ldots, 6$ (e.g. Beutler 2005):

$$\begin{aligned}\mathbf{r}_0(t_0) &\stackrel{\text{def}}{=} \mathbf{r}_0(t_0;\, E_1^0, E_2^0, \ldots, E_6^0)\,;\\ \dot{\mathbf{r}}_0(t_0) &\stackrel{\text{def}}{=} \mathbf{v}_0(t_0;\, E_1^0, E_2^0, \ldots, E_6^0).\end{aligned} \tag{2}$$

The particular choice of orbital elements is not important for our purpose. It is only important that the set chosen actually defines the initial values. Subsequently, we will refer to the solution $\mathbf{r}_0(t)$ as the reference orbit.

Let us now consider a second particular solution $\mathbf{r}(t)$ of Eq. 1, which is defined by a set of initial osculating elements E_k, $k = 1, 2, \ldots, 6$:

$$\begin{aligned}\mathbf{r}(t_0) &\stackrel{\text{def}}{=} \mathbf{r}(t_0;\, E_1, E_2, \ldots, E_6)\,;\\ \dot{\mathbf{r}}(t_0) &\stackrel{\text{def}}{=} \mathbf{v}(t_0;\, E_1, E_2, \ldots, E_6)\,,\end{aligned} \tag{3}$$

where we put

$$E_k \stackrel{\text{def}}{=} E_k^0 + \Delta E_k\,, \quad k = 1, 2, \ldots, 6\,. \tag{4}$$

From now on, we will assume that the differences ΔE_k are small quantities (as is usually done when dealing with non-linear LSQ problems), allowing us to neglect terms of higher than first-order. Under these assumptions, we are allowed to write:

$$\mathbf{r}(t) = \mathbf{r}_0(t) + \sum_{k=1}^{6} \mathbf{z}_k(t) \cdot \Delta E_k\,, \tag{5}$$

where

$$\mathbf{z}_k(t) \stackrel{\text{def}}{=} \frac{\partial \mathbf{r}_0(t)}{\partial E_k}\,, \quad k = 1, 2, \ldots, 6\,. \tag{6}$$

The function $\mathbf{z}_k(t)$ solves the so-called variational equation w.r.t. parameter E_k (e.g. Beutler 2005), which is obtained by taking the partial derivative of Eq. 1 for the reference orbit $\mathbf{r}_0(t)$ w.r.t. the initial osculating elements E_k:

$$\ddot{\mathbf{z}}_k = \mathbf{A}_0(t)\,\mathbf{z}_k + \mathbf{A}_1(t)\,\dot{\mathbf{z}}_k\,, \quad k = 1, 2, \ldots, 6\,, \tag{7}$$

where the 3×3 matrices $\mathbf{A}_i(t)$ are the Jacobian matrices of the deterministic function $\mathbf{f}(t) \stackrel{\text{def}}{=} \mathbf{f}(\mathbf{r}, \dot{\mathbf{r}}, t)$ w.r.t. the components of the geocentric position and velocity vectors of the satellite's reference orbit at time t.

Each function $\mathbf{z}_k(t)$, $k = 1, 2, \ldots, 6$, solves the same linear and homogeneous variational equation in Eq. 7. The initial values corresponding to different osculating elements E_k are, however, different. They are obtained by taking the partial derivatives of the initial values in Eq. 2 of the equation of motion w.r.t. the initial osculating elements:

$$\mathbf{z}_k(t_0) \stackrel{\text{def}}{=} \frac{\partial \mathbf{r}_0}{\partial E_k}\,; \quad \dot{\mathbf{z}}_k(t_0) \stackrel{\text{def}}{=} \frac{\partial \mathbf{v}_0}{\partial E_k}\,, \quad k = 1, 2, \ldots, 6. \tag{8}$$

The ensemble of the six functions $\mathbf{z}_k(t)$, $k = 1, 2, \ldots, 6$, forms a complete system of solutions of Eq. 7. Any solution of the variational equation may thus be written as a linear combination (with constant coefficients) of these six functions. Subsequently, we will make use of this property.

Several parameter estimation problems, all of which may be called orbit determination problems, will be solved subsequently. For this purpose, one needs observations o'_l, which are in the simplest case—apart from observation errors—the values of an observed function $o(\mathbf{r}(t_l))$ of the geocentric position vectors at the observation times t_l:

$$o'_l + \varepsilon_l = o(\mathbf{r}(t_l))\,; \quad l = 1, 2, \ldots, n_\mathrm{o}\,, \tag{9}$$

where ε_l is the observation error of observation o'_l and n_o the number of observations. If the observation errors have the expectation value of zero, we may use LSQ to determine the unbiased estimate of the unknown parameters and of the observation errors (called residuals in this context). Below, we will use the symbol ρ_l for the residuals (i.e. LSQ estimate of the observation error ε_l).

More complicated functions might be considered as observed functions (also involving, e.g. the velocities, or even positions and velocities referring to more than one epoch). The complications associated with such generalizations do not matter for our purpose; they would merely affect the actual form of the linearized relationship between observed functions and unknown parameters, which, according to Strang and Borre (1997) or any textbook on LSQ, just read as follows in the case of the observations of the type in Eq. 9:

$$\sum_{k=1}^{6} \frac{\partial o(\mathbf{r}_0(t_l))}{\partial E_k} \cdot \Delta E_k - \Delta\phi_l = \rho_l\,; \quad l = 1, 2, \ldots, n_\mathrm{o}\,, \tag{10}$$

where n_o is the number of observations, and the term

$$\Delta\phi_l \stackrel{\text{def}}{=} o'_l - o(\mathbf{r}_0(t_l)) \tag{11}$$

is also referred to as "observed minus computed".

The partial derivatives in the linearized Eqs. 10 may be expressed with the functions $\mathbf{z}_k(t)$ defined by Eqs. 6:

$$\frac{\partial o(\mathbf{r}_0(t_l))}{\partial E_k} = [\nabla o(\mathbf{r}_0(t_l))]^\mathrm{T} \cdot \mathbf{z}_k(t_l)\,, \tag{12}$$

where the gradient is defined by

$$\begin{aligned}[\nabla o(\mathbf{r}_0(t_l))]^\mathrm{T} &= \\ &= \left(\frac{\partial o(\mathbf{r}_0)}{\partial r_{0,1}}(t_l)\;\; \frac{\partial o(\mathbf{r}_0)}{\partial r_{0,2}}(t_l)\;\; \frac{\partial o(\mathbf{r}_0)}{\partial r_{0,3}}(t_l)\right).\end{aligned} \tag{13}$$

The gradient depends on the actual type of function observed (distances, angles, etc.), whereas the functions $\mathbf{z}_k(t)$, defined by Eqs. 7 and 8, do not depend on the observation type.

Orbit determination in its simplest form consists of the estimation of the six osculating elements in Eq. 3 using $n_\mathrm{o} \geq 6$ observations o'_l in a LSQ process. In matrix form, the following normal equation system of dimension six solves the problem:

$$\mathbf{A}^{\mathrm{T}}\mathbf{P}\mathbf{A}\cdot\Delta\mathbf{E}=\mathbf{A}^{\mathrm{T}}\mathbf{P}\Delta\boldsymbol{\phi}\ , \tag{14}$$

or, in abbreviated form:

$$\mathbf{N}\cdot\Delta\mathbf{E}=\mathbf{b}\ , \tag{15}$$

where $\mathbf{A}$ is the first design matrix with n_{o} lines and six columns (with $A_{lk}\stackrel{\mathrm{def}}{=}\partial o(\mathbf{r}_0(t_l))/\partial E_k$), $\Delta\mathbf{E}$ the vector containing the six increments of the orbital elements and $\Delta\phi$ the vector containing the terms "observed minus computed". $\mathbf{P}$ is the weight matrix. We will always assume a diagonal weight matrix in this article, in which case the diagonal elements of $\mathbf{P}$ are inversely proportional to the variances of the observations.

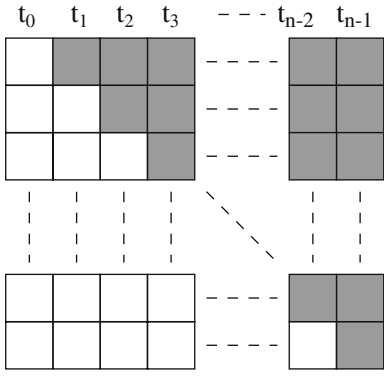

Fig. 1 Activity intervals of pseudo-stochastic pulses set up at epochs t_i, $i=1,2,\ldots,n-1$

3 Conventional estimation of pseudo-stochastic pulses

Pseudo-stochastic pulses are meant to absorb the effects of an insufficiently known force field or events like thruster firings, or any other model deficiency. They represent instantaneous velocity changes of size Δv_{ij}, $j=1,2,3$ at the epochs t_i, $i=1,2,\ldots,n-1$ in the pre-determined directions defined by the unit vectors $\mathbf{e}_{ij}$ (e.g. in radial, along-track and out-of-plane [cross-track] directions). A maximum of three pseudo-stochastic pulses may be set up at an epoch t_i (indicated by the index j). The complete time interval considered (integration interval or arc length) is assumed to be $I=[t_0,t_n]$.

The orbit determination problem making use of pseudo-stochastic pulses models a trajectory $\mathbf{r}(t)$ in the interval I by one set of initial conditions referring to the initial epoch t_0 and (at maximum) $3(n-1)$ pseudo-stochastic pulses Δv_{ij}, $j=1,2,3$ set up at the epochs t_i, $i=1,2,\ldots,n-1$. The resulting orbit $\mathbf{r}(t)$ is continuous in the entire interval, but the velocities $\dot{\mathbf{r}}(t)$ are discontinuous at the epochs t_i (i.e. "jumps" of size $|\Delta v_{ij}|$ in the directions $\mathbf{e}_{ij}$ at times t_i).

For $t\geq t_i$, the partial derivative $\mathbf{z}_{ij}(t)$ of the reference orbit $\mathbf{r}_0(t)$ w.r.t. the parameter Δv_{ij} is also a solution of Eq. 7. In view of the fact that each solution of Eq. 7 may be written as a linear combination (with constant coefficients) of the six solutions $\mathbf{z}_k(t)$, $k=1,2,\ldots,6$, referring to the six initial osculating elements, the partial derivatives w.r.t. the pseudo-stochastic pulses may be brought into the form

$$\mathbf{z}_{ij}(t)=\begin{cases}\mathbf{0} & t<t_i\\ \sum\limits_{k=1}^{6}\beta_{ij,k}\cdot\mathbf{z}_k(t) & t\geq t_i\end{cases}\ . \tag{16}$$

The above result is important: independent of the number of pseudo-stochastic pulses, we need only the six partial derivatives corresponding to the six initial osculating elements for the computation of the partial derivatives $\mathbf{z}_{ij}(t)$ w.r.t. all the pulses Δv_{ij}, $i=1,2,\ldots,n-1$, $j=1,2,3$. The coefficients $\beta_{ij,k}$ are obtained from the condition equations

$$\mathbf{z}_{ij}(t_i)=\mathbf{0}\ ;\quad \dot{\mathbf{z}}_{ij}(t_i)=\mathbf{e}_{ij}\ . \tag{17}$$

From the construction of Eq. 16, we may conclude that the coefficients have the following meaning:

$$\beta_{ij,k}=\frac{\partial E_k}{\partial\Delta v_{ij}}\ . \tag{18}$$

Let us also note, for later use, that the change of the initial osculating elements induced by the velocity change Δv_{ij} at t_i may be calculated as

$$\Delta E_{k,ij}=\frac{\partial E_k}{\partial\Delta v_{ij}}\cdot\Delta v_{ij}=\beta_{ij,k}\cdot\Delta v_{ij}\ . \tag{19}$$

Equation 16 says that the partial derivatives of the orbit w.r.t. Δv_{ij} are in general non-zero for $t>t_i$. This implies that the number of active parameters (i.e. with coefficients different from zero) in the observation equations (and the resulting normal equations) grows roughly linearly with time $|t-t_0|$. Figure 1 illustrates this growth of active parameters: The time intervals for which the stochastic parameters set up at a particular epoch t_i are active, i.e. the time interval where the partial derivatives $\mathbf{z}_{ij}(t)$, $j=1,2,3$, assume values different from zero, are shown in grey. From originally zero active pseudo-stochastic parameters in the subinterval $[t_0,t_1)$, this number grows to $3(n-1)$ in the last subinterval $[t_{n-1},t_n]$. This circumstance implies that the storage requirements grow with $|t_n-t_0|^2$ and the CPU requirements with $|t_n-t_0|^3$ (because of the dimension of the matrix to be inverted).

4 Pseudo-stochastic pulses: efficient method 1

In order to streamline the parameter estimation process, we have to study the structure of the observation equations. They contain the same terms related to the osculating elements as those in Eq. 10 and, in addition, the terms corresponding to the pseudo-stochastic pulses:

$$\sum_{k=1}^{6}\frac{\partial o(\mathbf{r}_0(t_l))}{\partial E_k}\cdot\Delta E_k+\sum_{m=1}^{i}\sum_{j=1}^{3}\frac{\partial o(\mathbf{r}_0(t_l))}{\partial\Delta v_{mj}}\cdot\Delta v_{mj}-\Delta\phi_l=\rho_l\ , \tag{20}$$

where the assumption was made that $t_l\in[t_i,t_{i+1})$ and that three pulses were set up per epoch. The partial derivatives

associated with the initial osculating elements may be represented by the scalar products in Eq. 12.

In an analogous way, the partial derivatives associated with the pseudo-stochastic pulses may be written as the following scalar products:

$$\frac{\partial o(\mathbf{r}_0(t_l))}{\partial \Delta v_{mj}} = \nabla\,(o(\mathbf{r}_0(t_l)))^{\mathrm{T}} \cdot \mathbf{z}_{mj}(t_l) = \nabla\,(o(\mathbf{r}_0(t_l)))^{\mathrm{T}} \cdot \sum_{k=1}^{6} \beta_{mj,k} \cdot \mathbf{z}_k(t_l). \quad (21)$$

The latter equality results when using Eq. 16 for the partial derivatives. Using Eqs. 12 and 21, the observation equation (Eq. 20) pertaining to observation l may thus be written:

$$\sum_{k=1}^{6} \nabla\,(o(\mathbf{r}_0(t_l)))^{\mathrm{T}} \cdot \mathbf{z}_k(t_l) \cdot \left\{ \Delta E_k + \sum_{m=1}^{i} \sum_{j=1}^{3} \beta_{mj,k} \cdot \Delta v_{mj} \right\} - \Delta\phi_l = \rho_l. \quad (22)$$

Let us now write all observation equations of the subinterval $[t_i, t_{i+1})$ in matrix notation:

$$\mathbf{A}_i \cdot \Delta\mathbf{E} + \mathbf{A}_i \cdot \sum_{m=1}^{i} \mathbf{B}_m \cdot \Delta\mathbf{v}_m - \boldsymbol{\Delta\phi}_i = \boldsymbol{\rho}_i, \quad (23)$$

where all matrices may be understood from comparing Eqs. 22 and 23. Let us note in particular:

$$\mathbf{B}_m = \begin{pmatrix} \beta_{m1,1} & \beta_{m2,1} & \beta_{m3,1} \\ \beta_{m1,2} & \beta_{m2,2} & \beta_{m3,2} \\ \dots & \dots & \dots \\ \dots & \dots & \dots \\ \beta_{m1,6} & \beta_{m2,6} & \beta_{m3,6} \end{pmatrix} \quad ; \quad \Delta\mathbf{v}_m = \begin{pmatrix} \Delta v_{m1} \\ \Delta v_{m2} \\ \Delta v_{m3} \end{pmatrix} . \quad (24)$$

Using Eq. 23 for the observation equations pertaining to the subintervals $[t_i, t_{i+1})$, $i = 0, 1, 2, \dots, n-1$, of the complete resulting normal equation system may be written as

$$\begin{pmatrix} \mathbf{A}^{\mathrm{T}}\mathbf{P}\mathbf{A} & \sum_{i=1}^{n-1} \mathbf{N}_i\,\mathbf{B}_1 & \dots & \sum_{i=n-1}^{n-1} \mathbf{N}_i\,\mathbf{B}_{n-1} \\ \dots & \mathbf{B}_1^{\mathrm{T}} \sum_{i=1}^{n-1} \mathbf{N}_i\,\mathbf{B}_1 & \dots & \mathbf{B}_1^{\mathrm{T}} \sum_{i=n-1}^{n-1} \mathbf{N}_i\,\mathbf{B}_{n-1} \\ \dots & \dots & \dots & \dots \\ \dots & \dots & \dots & \dots \\ \dots & \dots & \dots & \mathbf{B}_{n-1}^{\mathrm{T}} \sum_{i=n-1}^{n-1} \mathbf{N}_i\,\mathbf{B}_{n-1} \end{pmatrix} \cdot \begin{pmatrix} \Delta\mathbf{E} \\ \Delta\mathbf{v}_1 \\ \Delta\mathbf{v}_2 \\ \dots \\ \dots \\ \Delta\mathbf{v}_{n-1} \end{pmatrix} = \begin{pmatrix} \mathbf{A}^{\mathrm{T}}\mathbf{P}\boldsymbol{\Delta\phi} \\ \mathbf{B}_1^{\mathrm{T}} \sum_{i=1}^{n-1} \mathbf{A}_i^{\mathrm{T}}\mathbf{P}_i \cdot \boldsymbol{\Delta\phi}_i \\ \mathbf{B}_2^{\mathrm{T}} \sum_{i=2}^{n-1} \mathbf{A}_i^{\mathrm{T}}\mathbf{P}_i \cdot \boldsymbol{\Delta\phi}_i \\ \dots \\ \dots \\ \mathbf{B}_{n-1}^{\mathrm{T}} \sum_{i=n-1}^{n-1} \mathbf{A}_i^{\mathrm{T}}\mathbf{P}_i \cdot \boldsymbol{\Delta\phi}_i \end{pmatrix}, \quad (25)$$

where $\mathbf{N}_i = \mathbf{A}_i^{\mathrm{T}}\mathbf{P}_i\mathbf{A}_i$ and $\mathbf{A}^{\mathrm{T}}\mathbf{P}\mathbf{A} \overset{\text{def}}{=} \sum_{l=0}^{n-1} \mathbf{A}_l^{\mathrm{T}}\mathbf{P}_l\mathbf{A}_l$ is the normal equation matrix of the underlying deterministic problem, $\mathbf{A}^{\mathrm{T}}\mathbf{P}\Delta\phi \overset{\text{def}}{=} \sum_{i=0}^{n-1} \mathbf{A}_i^{\mathrm{T}}\mathbf{P}_i \cdot \boldsymbol{\Delta\phi}_i$, $\mathbf{P}_i$ is the weight matrix associated with the observations in interval $[t_i, t_{i+1})$, $\mathbf{A}_i^{\mathrm{T}}\mathbf{P}_i\mathbf{A}_i$ is that part of the normal equation matrix related to the six orbit parameters and same interval and $\mathbf{A}_i^{\mathrm{T}}\mathbf{P}_i \cdot \boldsymbol{\Delta\phi}_i$ is the right-hand side of the normal equation matrix (related to the six osculating elements and the corresponding subinterval).

The complete normal equation system may thus be set up easily and efficiently:

- The full normal equation system may be constructed with matrices $\mathbf{B}_i$, $i = 1, 2, \dots, n-1$, and the contributions $\mathbf{A}_i^{\mathrm{T}}\mathbf{P}_i\mathbf{A}_i$, $\mathbf{A}_i^{\mathrm{T}}\mathbf{P}_i \cdot \boldsymbol{\Delta\phi}_i$ to the normal equation system (of dimension six) related to the six initial osculating elements and the subintervals $[t_i, t_{i+1})$, $i = 0, 1, \dots, n-1$.
- There are no matrices of large dimensions involved when setting up these matrices. The time saving effect—when compared to the conventional method—is enormous; see Sect. 10 for an illustration.
- The basic building blocks of the resulting full normal equation matrix on the left-hand side of Eq. 25 are the partial sums $\sum_{l=i}^{n-1} \mathbf{A}_l^{\mathrm{T}}\mathbf{P}_l\mathbf{A}_l$, $i = n-1, n-2, \dots, 1, 0$. As indicated by this sequence, these sums are best built up starting with $i = n-1$ and ending with $i = 0$.
- The sub-matrix in row and column $i = k = 0$ is the normal equation matrix $\mathbf{A}^{\mathrm{T}}\mathbf{P}\mathbf{A} \overset{\text{def}}{=} \sum_{l=0}^{n-1} \mathbf{A}_l^{\mathrm{T}}\mathbf{P}_l\mathbf{A}_l$ corresponding to the parameter estimation problem without pseudo-stochastic pulses (cf. Eq. 14).
- The sub-matrix in the first row and in column $i > 0$ is obtained by multiplying the partial sum $\sum_{l=i}^{n-1} \mathbf{A}_l^{\mathrm{T}}\mathbf{P}_l\mathbf{A}_l$ with matrix $\mathbf{B}_i$ (from the right) for $i = 1, 2, \dots, n-1$.
- The sub-matrix in column i and row $0 < k \leq i$ is then obtained by multiplying the matrix in the first row of the same column with $\mathbf{B}_k^{\mathrm{T}}$ (from the left).

The resulting full normal equation matrix is, by definition, symmetric. Similarly, simple rules allow the efficient computation of the right-hand side of the resulting full normal equation system in Eq. 25.

As compared to the conventional process of setting up the normal equation system (using Eq. 22 without considering the relationships between the coefficients) the saving of processing time is most significant. The gain in efficiency will be discussed in Sect. 10. We avoid, in essence, the multiplication of matrices of dimension $(6 + 3(n-1))n_{\mathrm{obs}}$, the dominant part of calculations when setting up the normal equation system in the conventional way. The resulting normal equation system of course is of the (large) dimension $d = 6 + 3(n-1)$ and has to be inverted.

4.1 A priori weights on the pseudo-stochastic pulses

Here we deal with the issue of bringing in the a priori knowledge of the parameters $\Delta\mathbf{v}_i$ in a LSQ environment. It is this process that makes the result of a conventional LSQ adjustment essentially identical with that of filters (in particular of Bayesian type).

The pulses $\Delta\mathbf{v}_i$, $i = 1, 2, \ldots, n-1$ were introduced as empirical parameters. The attribute pseudo-stochastic is justified, if a priori constraints are put on these parameters (or on linear combinations of them). In the LSQ environment, additional knowledge is introduced through artificial observations of these parameters, which constrain them to zero with a certain weight defined by the weight matrix $\mathbf{W}$. This matrix is a user-defined input variable of the algorithm. The actual choice is based (hopefully) on the knowledge of the deficiencies of the force field. The artificial observations referring to the epoch i read as

$$\Delta\mathbf{v}_i = \mathbf{0}\,. \tag{26}$$

The weight matrix $\mathbf{W}$ associated with these observations may be defined as the inverse of the variance–covariance matrix associated with these parameters:

$$\mathbf{W} \stackrel{\text{def}}{=} \sigma_0^2\ \mathbf{cov}\,(\Delta\mathbf{v}_i)^{-1} \stackrel{\text{def}}{=} \begin{pmatrix} \frac{\sigma_0^2}{\sigma_1^2} & 0 & 0 \\ 0 & \frac{\sigma_0^2}{\sigma_2^2} & 0 \\ 0 & 0 & \frac{\sigma_0^2}{\sigma_3^2} \end{pmatrix}\,, \tag{27}$$

where σ_0 is the a priori RMS error of the (real) observation of unit weight and where σ_k, $k = 1, 2, 3$, are the user-defined RMS errors associated with the three components of $\Delta\mathbf{v}_i$. It is assumed here (but this is in principle not relevant) that the weight matrices assigned to each of the pseudo-stochastic pulses are identical. This is why the weight matrix $\mathbf{W}$ does not require the subinterval index i. Note that it would be possible to assign a fully populated weight matrix to the artificial observations related to the epoch i.

The weight matrix $\mathbf{W}$ simply has to be superimposed on all diagonal matrices related to the pseudo-stochastic pulses before the inversion of Eq. 25:

$$\left[\mathbf{B}_i^{\mathrm{T}} \sum_{l=i}^{n-1} \mathbf{A}_l^{\mathrm{T}} \mathbf{P}_l \mathbf{A}_l\ \mathbf{B}_i\right]' \stackrel{\text{def}}{=} \mathbf{B}_i^{\mathrm{T}} \sum_{l=i}^{n-1} \mathbf{A}_l^{\mathrm{T}} \mathbf{P}_l \mathbf{A}_l\ \mathbf{B}_i + \mathbf{W}\,, \quad i = 1, 2, \ldots, n-1. \tag{28}$$

This superposition is not a time-consuming operation.

Let us note, as a side remark, that these artificial observations have to be treated like normal observations when calculating the mean error m_0 of the weight unit a posteriori. The number of observations $n_{\mathrm{obs,act}}$ to be considered by the LSQ method therefore consists of the sum of "real" and "artificial" observations:

$$n_{\mathrm{obs,act}} = n_{\mathrm{obs,real}} + 3(n-1)\,, \tag{29}$$

assuming that we always set up three pseudo-stochastic pulses per epoch t_i. The mean error a posteriori is thus computed as

$$m_0 = \sqrt{\frac{\sum_{i=0}^{n-1} \boldsymbol{\rho}_i^{\mathrm{T}}\ \mathbf{P}_i\ \boldsymbol{\rho}_i}{n_{\mathrm{obs,act}} - n_{\mathrm{p}}}}\,, \tag{30}$$

where $\boldsymbol{\rho}_i$ is the array of residuals in interval i and n_{p} the total number of parameters (including the pseudo-stochastic parameters). Remember that the numerator in the square root may be calculated as the difference of the (weighted) sum of the terms "observed minus computed" (replace $\boldsymbol{\rho}_i$ by $\Delta\phi_i$ in Eq. 30) and the scalar product of the array formed by the right-hand side of Eq. 25 and the (total) solution vector.

With Eqs. 26 and 27 we have defined the simplest possible stochastic model for the pseudo-stochastic parameters introduced, namely that of a white noise sequence. The constraints are "absolute" in the sense that the total deviation of the resulting trajectory (*not* of the a priori trajectory) is constrained to the "best fitting" deterministic orbit. If the orbit is improved iteratively, the total velocity change (of all iteration steps) and not only the increment estimated in the current step have to be constrained. Otherwise, convergence problems might occur.

We might also constrain the variation of the difference between subsequent parameter sets by artificial observations. We might call such parameters "relative constraints". When doing that, the resulting stochastic model for our parameters would be closely related to that of a random walk. In this paper, however, we will confine ourselves to the simplest model represented by Eqs. 26 and 27.

4.2 The case of additional parameters

Here we deal with the important aim to generalize the orbit determination problem, by allowing for more than six (deterministic) orbit parameters, more than one satellite and other (than orbit-related) parameter types. The problem is rather of a technical and not of a fundamental character. Readers only interested in the key elements of the efficient algorithms may therefore proceed directly to Sect. 5.

Generalizations, which are either due to dynamical systems governed by differential equation systems of order $n \neq 2$, the dimension $d \neq 3$, or which are due to additional deterministic orbit parameters (e.g. associated with radiation pressure or atmospheric drag models containing adjustable parameters, in the simplest case scaling factors), are trivial and need not be considered further.

The simple case considered so far is actually important in practice. It occurs, e.g. when using the Cartesian coordinates of LEO positions (e.g. established with kinematic methods) as "observations" (Beutler 2005) or when analysing the GPS code observations of a spaceborne receiver (after pre-elimination of the spaceborne receiver's clock parameters).

More general problems occur in practice, however. Our algorithms, in order to be really useful, have to cope with them. Let us mention two important cases:

- When estimating an orbit (parameterized with initial osculating elements and pseudo-stochastic pulses) using the GPS carrier-phase observations of the LEO receiver, one has to cope with the ambiguity parameters (associated with the phase measurements of the spaceborne receiver) in addition to the orbit parameters. The number of ambiguity parameters may be considerable and outnumber the other parameters.
- The situation becomes even more complicated if double-difference GPS carrier-phase observations of the spaceborne GPS receiver are processed together with those of a terrestrial network of GPS receivers. The ambiguity parameters related to the entire ensemble of ground- and space-based GPS receivers, the troposphere parameters related to ground tracking sites, possibly even the coordinates of these sites, etc. may appear in the observation equations in addition to the deterministic and pseudo-stochastic orbit parameters.

It is, in principle, simple to cope with such cases: the additional parameters may formally be considered as deterministic orbit parameters. This implies that the dimension of the square matrices $\mathbf{A}_i^{\mathrm{T}}\mathbf{P}_i\mathbf{A}_i$ is no longer six, but (much) larger. Depending on the specific problem, this may mean that the "efficient" procedure outlined in Sect. 4 becomes inefficient, because the efficiency really is due to the fact that the dimension of the matrices related to the subintervals is small.

The solution of the problem may be written in simple form by introducing the following generalized array of parameters:

$$\Delta\tilde{\mathbf{E}}^{\mathrm{T}} \stackrel{\mathrm{def}}{=} \left(\Delta\mathbf{E}^{\mathrm{T}},\, p_1,\, p_2,\, \ldots,\, p_{\tilde{n}}\right), \tag{31}$$

where $\tilde{n}$ is the number of additional parameters p_i (dynamical orbit parameters and others, like ambiguity parameters), and the generalized coefficient matrix

$$\tilde{\mathbf{B}}_m = \begin{pmatrix} \beta_{m1,1} & \beta_{m2,1} & \beta_{m3,1} \\ \beta_{m1,2} & \beta_{m2,2} & \beta_{m3,2} \\ \cdots & \cdots & \cdots \\ \cdots & \cdots & \cdots \\ \beta_{m1,6} & \beta_{m2,6} & \beta_{m3,6} \\ 0 & 0 & 0 \\ \cdots & \cdots & \cdots \\ \cdots & \cdots & \cdots \\ 0 & 0 & 0 \end{pmatrix}, \tag{32}$$

where the number of "zero-rows" equals the number $\tilde{n}$ of additional parameters. With these definitions, the solution of the general problem may be written in the form:

$$\begin{pmatrix} \tilde{\mathbf{A}}^{\mathrm{T}}\mathbf{P}\tilde{\mathbf{A}} & \sum_{i=1}^{n-1}\tilde{\mathbf{N}}_i\,\tilde{\mathbf{B}}_1 & \ldots & \sum_{i=n-1}^{n-1}\tilde{\mathbf{N}}_i\,\tilde{\mathbf{B}}_{n-1} \\ \ldots & \tilde{\mathbf{B}}_1^{\mathrm{T}}\sum_{i=1}^{n-1}\tilde{\mathbf{N}}_i\,\tilde{\mathbf{B}}_1 & \ldots & \tilde{\mathbf{B}}_1^{\mathrm{T}}\sum_{i=n-1}^{n-1}\tilde{\mathbf{N}}_i\,\tilde{\mathbf{B}}_{n-1} \\ \ldots & \ldots & \ldots & \ldots \\ \ldots & \ldots & \ldots & \ldots \\ \ldots & \ldots & \ldots & \tilde{\mathbf{B}}_{n-1}^{\mathrm{T}}\sum_{i=n-1}^{n-1}\tilde{\mathbf{N}}_i\,\tilde{\mathbf{B}}_{n-1} \end{pmatrix} \cdot \begin{pmatrix} \Delta\tilde{\mathbf{E}} \\ \Delta\mathbf{v}_1 \\ \Delta\mathbf{v}_2 \\ \ldots \\ \ldots \\ \Delta\mathbf{v}_{n-1} \end{pmatrix} = \begin{pmatrix} \tilde{\mathbf{A}}^{\mathrm{T}}\mathbf{P}\Delta\boldsymbol{\phi} \\ \tilde{\mathbf{B}}_1^{\mathrm{T}}\sum_{i=1}^{n-1}\tilde{\mathbf{A}}_i^{\mathrm{T}}\mathbf{P}_i\cdot\Delta\boldsymbol{\phi}_i \\ \tilde{\mathbf{B}}_2^{\mathrm{T}}\sum_{i=2}^{n-1}\tilde{\mathbf{A}}_i^{\mathrm{T}}\mathbf{P}_i\cdot\Delta\boldsymbol{\phi}_i \\ \ldots \\ \ldots \\ \tilde{\mathbf{B}}_{n-1}^{\mathrm{T}}\sum_{i=n-1}^{n-1}\tilde{\mathbf{A}}_i^{\mathrm{T}}\mathbf{P}_i\cdot\Delta\boldsymbol{\phi}_i \end{pmatrix}, \tag{33}$$

where $\tilde{\mathbf{N}}_i = \tilde{\mathbf{A}}_i^{\mathrm{T}}\mathbf{P}_i\tilde{\mathbf{A}}_i$ and the first design matrices $\tilde{\mathbf{A}}_i^{\mathrm{T}}$ contain the matrices $\mathbf{A}_i^{\mathrm{T}}$ and the terms due to the new parameters (partial derivatives w.r.t. the new parameters).

The efficient computation of Eq. 33 follows the same pattern as in the simpler case in Eq. 25: the partial sums $\sum_{i=k}^{n-1}\tilde{\mathbf{A}}_i^{\mathrm{T}}\mathbf{P}_i\tilde{\mathbf{A}}_i$, $k = n-1, n-2, \ldots, 0$ are calculated first, then these sums are multiplied from the right with matrices $\tilde{\mathbf{B}}_k$ for $k = 1, 2, \ldots, n-1$. These results are in turn multiplied from the left with $\tilde{\mathbf{B}}_l^{\mathrm{T}}$, $l = 1, 2, \ldots, k$.

Whether or not the procedure is efficient depends on:

1. The dimensions of the terms of the partial sums
2. The dimensions of the partial sums

The dimensions of the terms of the partial sums and the dimensions of all partial sums are the same if the newly added parameters occur in each of the subintervals $[t_i, t_{i+1})$, $i = 0, 1, \ldots, n-1$. This is the case if only dynamical parameters (e.g. related to a radiation pressure model) have been set up. In this case, and if the number of additional parameters is large (of the order of the number of pseudo-stochastic parameters), the algorithm inevitably becomes inefficient because the matrix operations are all related to matrices of large dimensions.

Other parameters, e.g. the ambiguities, occur only during comparatively short time intervals (individual ambiguities only show up in few consecutive subintervals). Under these circumstances, the dimensions of the terms in the partial sums are much smaller than the dimension of the entire system. The solution method is still very efficient, when compared to the conventional method. We refer to Sect. 10 for quantitative information on this statement.

5 Pseudo-stochastic pulses: efficient method 2

In this section, we develop a second, even more efficient method than in Sect. 4, which avoids the setting up and inver-

sion of the full normal equation matrix Eq. 25. The only drawback resides in the fact that the full variance–covariance matrix of this second solution is not available. The solutions of methods 1 and 2 are, however, algebraically identical. The variance–covariance matrix of the (usually six) deterministic orbit parameters and of each of the pseudo-stochastic pulses $\Delta\mathbf{v}_i$ is available and algebraically identical with the corresponding information of the previous method. Those parts of the full variance–covariance matrix, which describe either the correlations between the initial osculating elements and the pulses or the correlations between the pulses referring to different epochs, are not available.

The development of the second method starts from Eq. 22, where we only allow for the six deterministic and the $3(n-1)$ pseudo-stochastic parameters. We do not consider more general problems in this section in order not to overload the formalism. For an observation performed at $t_l \in [t_i, t_{i+1})$, the observation equation reads:

$$\sum_{k=1}^{6} \nabla\,(o(\mathbf{r}_0(t_l)))^{\mathrm{T}} \cdot \mathbf{z}_k(t_l) \cdot \Bigg\{ \Delta E_k + \sum_{m=1}^{i} \sum_{j=1}^{3} \beta_{mj,k} \cdot \Delta v_{mj} \Bigg\} - \Delta\phi_l = \rho_l. \tag{34}$$

The scalar term in the brackets $\{\cdots\}$ in Eq. 34 has a very simple meaning: the element defined by $E_k^i \stackrel{\text{def}}{=} E_k^0 + \{\cdots\}$ is the osculating element k at t_0 defining the solution $\mathbf{r}(t)$ in the subinterval $[t_i, t_{i+1})$. Therefore, Eq. 34 may also be written as

$$\sum_{k=1}^{6} \nabla\,(o(\mathbf{r}_0(t_l)))^{\mathrm{T}} \cdot \mathbf{z}_k(t_l) \cdot \Delta E_k^i - \Delta\phi_l = \rho_l. \tag{35}$$

Equation 35 states that the problem of determining an orbit with six initial osculating elements $E_k^0 + \Delta E_k$, $k = 1, 2, \ldots, 6$ and (any number of) pseudo-stochastic pulses Δv_{mj} may be parameterized within each of the subintervals $[t_i, t_{i+1})$, $i = 0, 1, \ldots, n-1$ by only six quantities, namely the osculating elements at t_0 characterizing the trajectory within the particular subinterval!

In order to exploit this important property, we have to perform the parameter transformation $\Delta E_k^{i-1} \rightarrow \Delta E_k^i$ at each of the epochs t_i (the subinterval boundaries), after having set up the normal equation system containing all observations up to the epoch t_i. The change of the osculating elements from interval $[t_{i-1}, t_i)$ to interval $[t_i, t_{i+1})$ is caused by the three pulses Δv_{ij}, $j = 1, 2, 3$ at the epoch t_i. In view of Eq. 19 we may therefore write:

$$\Delta E_k^i \stackrel{\text{def}}{=} \Delta E_k^{i-1} + \sum_{j=1}^{3} \beta_{ij,k} \cdot \Delta v_{ij}\ ,\ k = 1, 2, \ldots, 6\ . \tag{36}$$

These transformation equations may be written in convenient matrix form

$$\Delta\mathbf{E}_i \stackrel{\text{def}}{=} \Delta\mathbf{E}_{i-1} + \mathbf{B}_i \cdot \Delta\mathbf{v}_i\ , \tag{37}$$

where $\Delta\mathbf{E}_{i-1}$ and $\Delta\mathbf{E}_i$ are the column matrices containing the elements ΔE_k^{i-1} and ΔE_k^i, $k = 1, 2, \ldots, 6$, respectively. Matrix $\mathbf{B}_i$ is defined by Eq. 24. Formally, the array $\Delta\mathbf{E}_{i-1}$ may thus be written as a function of the arrays $\Delta\mathbf{E}_i$ and $\Delta\mathbf{v}_i$:

$$\Delta\mathbf{E}_{i-1} = \left(\mathbf{I}_6 - \mathbf{B}_i\right) \cdot \begin{pmatrix} \Delta\mathbf{E}_i \\ \Delta\mathbf{v}_i \end{pmatrix}\ , \tag{38}$$

where $\mathbf{I}_6$ is the unit matrix of dimension six.

Let us now assume that the normal equation system containing the contributions of all observations made before t_i may be written in the following form:

$$\mathbf{N}_{i-1} \cdot \Delta\mathbf{E}_{i-1} = \mathbf{b}_{i-1}\ , \tag{39}$$

where

$$\begin{aligned} \mathbf{N}_{i-1} &\stackrel{\text{def}}{=} \mathbf{A}_{i-1}^{\mathrm{T}} \mathbf{P}_{i-1} \mathbf{A}_{i-1} \\ \mathbf{b}_{i-1} &\stackrel{\text{def}}{=} \mathbf{A}_{i-1}^{\mathrm{T}} \mathbf{P}_{i-1} \Delta\boldsymbol{\phi}_{i-1}\ , \quad i = 1, \end{aligned} \tag{40}$$

and

$$\begin{aligned} \mathbf{N}_{i-1} &\stackrel{\text{def}}{=} \mathbf{N}_{i-2}^{*} + \mathbf{A}_{i-1}^{\mathrm{T}} \mathbf{P}_{i-1} \mathbf{A}_{i-1}\ , \\ \mathbf{b}_{i-1} &\stackrel{\text{def}}{=} \mathbf{b}_{i-2}^{*} + \mathbf{A}_{i-1}^{\mathrm{T}} \mathbf{P}_{i-1} \Delta\boldsymbol{\phi}_{i-1}\ , \quad i > 1\ . \end{aligned} \tag{41}$$

For the precise definition of $\mathbf{N}_{i-2}^{*}$ and $\mathbf{b}_{i-2}^{*}$, see Eqs. 48 and 49.

We include here, for the sake of completeness, the update procedure for the weighted sum of the terms "observed minus computed":

$$\sum_{k=0}^{i-1} \Delta\boldsymbol{\phi}_k^{\mathrm{T}} \mathbf{P}_k \Delta\boldsymbol{\phi}_k \stackrel{\text{def}}{=} \Delta\boldsymbol{\phi}_{i-1}^{\mathrm{T}} \mathbf{P}_{i-1} \Delta\boldsymbol{\phi}_{i-1}\ , \quad i = 1 \tag{42}$$

and

$$\sum_{k=0}^{i-1} \Delta\boldsymbol{\phi}_k^{\mathrm{T}} \mathbf{P}_k \Delta\boldsymbol{\phi}_k \stackrel{\text{def}}{=} \left(\sum_{k=0}^{i-2} \Delta\boldsymbol{\phi}_k^{\mathrm{T}} \mathbf{P}_k \Delta\boldsymbol{\phi}_k \right)^{*} + \Delta\boldsymbol{\phi}_{i-1}^{\mathrm{T}} \mathbf{P}_{i-1} \Delta\boldsymbol{\phi}_{i-1}\ , \quad i > 1\ . \tag{43}$$

Using Eq. 38, Eq. 39 may be transformed into a system in the unknowns $\Delta\mathbf{E}_i$ and $\Delta\mathbf{v}_i$ by replacing $\Delta\mathbf{E}_{i-1}$ on the left-hand side by $\Delta\mathbf{E}_i$ and $\Delta\mathbf{v}_i$, and by multiplying (from the left) both sides of Eq. 39 with the transpose of the transformation matrix $(\mathbf{I}_6 - \mathbf{B}_i)$ in Eq. 38:

$$\begin{pmatrix} \mathbf{N}_{i-1} & -\mathbf{N}_{i-1}\mathbf{B}_i \\ -\mathbf{B}_i^{\mathrm{T}}\mathbf{N}_{i-1} & \mathbf{B}_i^{\mathrm{T}}\mathbf{N}_{i-1}\mathbf{B}_i \end{pmatrix} \cdot \begin{pmatrix} \Delta\mathbf{E}_i \\ \Delta\mathbf{v}_i \end{pmatrix} = \begin{pmatrix} \mathbf{b}_{i-1} \\ -\mathbf{B}_i^{\mathrm{T}}\,\mathbf{b}_{i-1} \end{pmatrix}\ . \tag{44}$$

The transformed normal equation system (Eq. 44) is the key to the efficient solution of our orbit determination problem: Eq. (35) tells that the observations contained in the interval $[t_i, t_{i+1})$ do not depend on the terms $\Delta\mathbf{v}_i$ explicitly—their influence is already taken into account by the array of osculating elements $\Delta\mathbf{E}_i$. As the same is true not only for the interval $[t_i, t_{i+1})$, but also for all subsequent subintervals $[t_{i+k}, t_{i+k+1})$, $k = 1, 2, \ldots, n-i-1$, we may as well pre-eliminate the terms $\Delta\mathbf{v}_i$ at t_i, immediately after having set them up. Observe that the pre-elimination is not possible

without performing the parameter transformation defined in Eq. 38.

Before doing that, we have to add the constraints related to the pulses $\Delta\mathbf{v}_i$ to Eq. 44:

$$\begin{pmatrix} \mathbf{N}_{i-1} & -\mathbf{N}_{i-1}\mathbf{B}_i \\ -\mathbf{B}_i^{\mathrm{T}}\mathbf{N}_{i-1} & \left[\mathbf{B}_i^{\mathrm{T}}\mathbf{N}_{i-1}\mathbf{B}_i\right]' \end{pmatrix} \cdot \begin{pmatrix} \Delta\mathbf{E}_i \\ \Delta\mathbf{v}_i \end{pmatrix} = \begin{pmatrix} \mathbf{b}_{i-1} \\ -\mathbf{B}_i^{\mathrm{T}}\,\mathbf{b}_{i-1} \end{pmatrix}, \tag{45}$$

where the term $\mathbf{B}_i^{\mathrm{T}}\mathbf{N}_{i-1}\mathbf{B}_i$ was modified in analogy to Eq. 28:

$$\left[\mathbf{B}_i^{\mathrm{T}}\mathbf{N}_{i-1}\mathbf{B}_i\right]' \stackrel{\text{def}}{=} \mathbf{B}_i^{\mathrm{T}}\mathbf{N}_{i-1}\mathbf{B}_i + \mathbf{W}. \tag{46}$$

We are now in a position to pre-eliminate the pulse $\Delta\mathbf{v}_i$. The result, uniquely derived from Eq. 45, may be written in the form:

$$\mathbf{N}_{i-1}^{*} \cdot \Delta\mathbf{E}_i = \mathbf{b}_{i-1}^{*}\,, \tag{47}$$

where

$$\mathbf{N}_{i-1}^{*} \stackrel{\text{def}}{=} \mathbf{N}_{i-1} - \mathbf{N}_{i-1}\mathbf{B}_i \left(\left[\mathbf{B}_i^{\mathrm{T}}\mathbf{N}_{i-1}\mathbf{B}_i\right]'\right)^{-1} \mathbf{B}_i^{\mathrm{T}}\mathbf{N}_{i-1} \tag{48}$$

and

$$\mathbf{b}_{i-1}^{*} \stackrel{\text{def}}{=} \mathbf{b}_{i-1} - \mathbf{N}_{i-1}\mathbf{B}_i \left(\left[\mathbf{B}_i^{\mathrm{T}}\mathbf{N}_{i-1}\mathbf{B}_i\right]'\right)^{-1} \mathbf{B}_i^{\mathrm{T}}\mathbf{b}_{i-1} \tag{49}$$

are obtained by pre-eliminating the term $\Delta\mathbf{v}_i$ from Eq. 45.

The weighted sum of the terms "observed minus computed" also has to be transformed:

$$\left(\sum_{k=0}^{i-1} \Delta\boldsymbol{\phi}_k^{\mathrm{T}}\mathbf{P}_k\Delta\boldsymbol{\phi}_k\right)^{*} \stackrel{\text{def}}{=} \sum_{k=0}^{i-1} \Delta\boldsymbol{\phi}_k^{\mathrm{T}}\mathbf{P}_k\Delta\boldsymbol{\phi}_k - \mathbf{b}_{i-1}^{\mathrm{T}}\mathbf{B}_i \left(\left[\mathbf{B}_i^{\mathrm{T}}\mathbf{N}_{i-1}\mathbf{B}_i\right]'\right)^{-1} \mathbf{B}_i^{\mathrm{T}}\mathbf{b}_{i-1}. \tag{50}$$

Having updated the normal equation system in the last subinterval using Eq. 41 for $i = n$, we may invert the resulting normal equation matrix $\mathbf{N}_{n-1}$ and solve for the orbital elements $\Delta\mathbf{E}_{n-1}$ (note that it is neither necessary nor possible to set up and pre-eliminate a pulse $\Delta\mathbf{v}_n$ at t_n):

$$\Delta\mathbf{E}_i = \mathbf{N}_i^{-1}\,\mathbf{b}_i \stackrel{\text{def}}{=} \mathbf{Q}_i\,\mathbf{b}_i\,, \quad i = n-1\,. \tag{51}$$

Observe that there was no need to calculate the other element sets $\Delta\mathbf{E}_i$, $i = 0, 1, \ldots, n-2$ explicitly in order to get the set of elements $\Delta\mathbf{E}_{n-1}$, although this would have been possible. The intermediate results would have been the filter solutions based on all observations in the interval $[t_0, t_{i+1})$, $i = 0, 1, \ldots, n-1$.

After having updated the weighted sum of the terms "observed minus computed" for $i = n$ using Eq. 43, we may compute the mean error a posteriori as

$$m_0 = \sqrt{\frac{\sum_{k=0}^{n-1} \Delta\boldsymbol{\phi}_k^{\mathrm{T}}\mathbf{P}_k\Delta\boldsymbol{\phi}_k - \Delta\mathbf{E}_{n-1}^{\mathrm{T}} \cdot \mathbf{b}_{n-1}}{n_{\mathrm{obs,act}} - (6 + 3(n-1))}}. \tag{52}$$

The a posteriori estimate of the variance–covariance matrix related to the osculating elements referring to the last interval $I_{n-1} \stackrel{\text{def}}{=} [t_{n-1}, t_n]$ is then calculated by

$$\mathbf{cov}\,(\Delta\mathbf{E}_{n-1}) = m_0^2 \cdot \mathbf{N}_{n-1}^{-1} = m_0^2 \cdot \mathbf{Q}_{n-1}. \tag{53}$$

Having established $\Delta\mathbf{E}_{n-1}$ and the covariance matrix associated with it, we may now invoke the back-substitution process. Equation 45, which was already used for the pre-elimination process, is again at the center of interest. In order to understand the back-substitution process, it is advisable to write down the normal equation system at the end of the last subinterval $[t_{n-1}, t_n]$, which would have resulted without pre-elimination of the pulses $\Delta\mathbf{v}_{n-1}$. This system is easily obtained from Eq. 45 for $i - 1 = n - 2$ by updating the first term $\mathbf{N}_{i-1}$ on the left-hand side and the first term on the right-hand side according to

$$\begin{aligned} \tilde{\mathbf{N}}_{i-1} &\stackrel{\text{def}}{=} \mathbf{N}_{i-2} + \mathbf{A}_{i-1}^{\mathrm{T}}\mathbf{P}_{i-1}\mathbf{A}_{i-1}\,, \\ \tilde{\mathbf{b}}_{i-1} &\stackrel{\text{def}}{=} \mathbf{b}_{i-2} + \mathbf{A}_{i-1}^{\mathrm{T}}\mathbf{P}_{i-1}\Delta\boldsymbol{\phi}_{i-1}\,, \end{aligned} \tag{54}$$

for $i = n$.

When comparing Eqs. 41 and 54, we see that the transformation in Eqs. 48 and 49 need not be performed if the pre-elimination is not performed. The resulting "full" normal equation system (with the term $\Delta\mathbf{v}_{n-1}$) at the end of the interval $[t_{n-1}, t_n]$ therefore reads

$$\begin{pmatrix} \tilde{\mathbf{N}}_i & -\mathbf{N}_{i-1}\mathbf{B}_i \\ -\mathbf{B}_i^{\mathrm{T}}\mathbf{N}_{i-1} & \left[\mathbf{B}_i^{\mathrm{T}}\mathbf{N}_{i-1}\mathbf{B}_i\right]' \end{pmatrix} \cdot \begin{pmatrix} \Delta\mathbf{E}_i \\ \Delta\mathbf{v}_i \end{pmatrix} = \begin{pmatrix} \tilde{\mathbf{b}}_i \\ -\mathbf{B}_i^{\mathrm{T}}\,\mathbf{b}_{i-1} \end{pmatrix}, \tag{55}$$

where $i = n - 1$.

By comparing Eqs. 55 and 45, we see that they only differ in the terms $\tilde{\mathbf{N}}_i$ (instead of $\mathbf{N}_{i-1}$) and $\tilde{\mathbf{b}}_i$ (instead of $\mathbf{b}_{i-1}$). From Eq. 55, we may easily calculate the pseudo-stochastic pulses (for $i = n - 1$) with quantities that are known by now, i.e. by circumventing the terms $\tilde{\mathbf{N}}_i$ and $\tilde{\mathbf{b}}_i$:

$$\Delta\mathbf{v}_i = \left\{\left[\mathbf{B}_i^{\mathrm{T}}\mathbf{N}_{i-1}\mathbf{B}_i\right]'\right\}^{-1} \left[\mathbf{B}_i^{\mathrm{T}}\mathbf{N}_{i-1}\Delta\mathbf{E}_i - \mathbf{B}_i^{\mathrm{T}}\mathbf{b}_{i-1}\right]. \tag{56}$$

Observe that all terms in Eq. 56—except $\Delta\mathbf{E}_i$ (which is known from Eq. 51)—are those already calculated in the update step for $i = n - 1$ (see Eq. 45).

In order to calculate the variance–covariance matrix associated with the pulse $\Delta\mathbf{v}_i$, we have to invert the normal equation matrix on the left-hand side of Eq. 55. Actually we do not need to perform the inversion, because we already know sub-matrix $\mathbf{Q}_i$ for $i = n - 1$ after having solved the reduced normal equation system by Eq. 51. We may therefore calculate the full inverse of the normal equation matrix by

$$\begin{pmatrix} \tilde{\mathbf{N}}_i & -\mathbf{N}_{i-1}\mathbf{B}_i \\ -\mathbf{B}_i^{\mathrm{T}}\mathbf{N}_{i-1} & \left[\mathbf{B}_i^{\mathrm{T}}\mathbf{N}_{i-1}\mathbf{B}_i\right]' \end{pmatrix} \cdot \begin{pmatrix} \mathbf{Q}_i & \mathbf{Q}_{i,12} \\ \mathbf{Q}_{i,12}^{\mathrm{T}} & \mathbf{Q}_{i,22} \end{pmatrix} = \begin{pmatrix} \mathbf{I}_6 & \mathbf{0} \\ \mathbf{0} & \mathbf{I}_3 \end{pmatrix}, \tag{57}$$

where $\mathbf{I}_k$, $k = 3, 6$ are the unit matrices of dimension k.

Making full use of the known sub-matrices in Eq. 57, we easily obtain the missing elements of the full inverse matrix, explicitly:

$$\mathbf{Q}_{i,12} = \mathbf{Q}_i\ \ (\mathbf{N}_{i-1}\mathbf{B}_i)\ \ \left\{\left[\mathbf{B}_i^{\mathrm{T}}\mathbf{N}_{i-1}\mathbf{B}_i\right]'\right\}^{-1} \tag{58}$$

and

$$\mathbf{Q}_{i,22} = \left\{\left[\mathbf{B}_i^{\mathrm{T}}\mathbf{N}_{i-1}\mathbf{B}_i\right]'\right\}^{-1} \left\{\mathbf{I}_3 + \mathbf{B}_i^{\mathrm{T}}\mathbf{N}_{i-1}\mathbf{Q}_{i,12}\right\}. \tag{59}$$

The variance–covariance matrix associated with pulse $\Delta\mathbf{v}_i$ (for $i = n-1$) may now be calculated as

$$\mathbf{cov}\,(\Delta\mathbf{v}_i) = m_0^2 \cdot \mathbf{Q}_{i,22} \tag{60}$$

Having evaluated $\Delta\mathbf{v}_{n-1}$ using Eq. 56 (with $i = n-1$), we may now calculate $\Delta\mathbf{E}_{n-2}$ using Eq. 38 for $i = n-1$. In view of Eq. 60, we obtain the associated variance–covariance matrix by

$$\mathbf{cov}\,(\Delta\mathbf{E}_{i-1}) = m_0^2 \cdot \begin{pmatrix} \mathbf{I}_6 & -\mathbf{B}_i \end{pmatrix} \cdot \begin{pmatrix} \mathbf{Q}_i & \mathbf{Q}_{i,12} \\ \mathbf{Q}_{i,12}^{\mathrm{T}} & \mathbf{Q}_{i,22} \end{pmatrix} \cdot \begin{pmatrix} \mathbf{I}_6 \\ -\mathbf{B}_i^{\mathrm{T}} \end{pmatrix}, \tag{61}$$

where $i = n-1$.

With Eqs. 38 and 61, we have established the solution vector $\Delta\mathbf{E}_{n-2}$ and the variance–covariance matrix associated with it. This means that we may now calculate the remaining sets of elements $\Delta\mathbf{E}_i$ and pulses $\Delta\mathbf{v}_i$ using the above equations with the appropriate indices i.

5.1 The case of additional parameters

In the development of our second method, we only took into account osculating elements and pseudo-stochastic pulses as parameters of the normal equation system. As already mentioned in Sect. 4.2, other parameter types (like ambiguity parameters, troposphere parameters, etc.) may show up in a "real" orbit determination environment.

The principles for the efficient solution remain the same. The difference resides merely in the fact that Eq. 44 contains additional parameters. The orbit determination process still consists of (a) a parameter transformation and a pre-elimination process (where not only the pseudo-stochastic pulses, but also other parameters, e.g. the ambiguities, which may or may not be pre-eliminated at the end of the subintervals) and (b) a back-substitution process.

This implies that we have to generalize Eq. 44 to contain a parameter array $\Delta\tilde{\mathbf{E}}_i$ that contains the array $\Delta\mathbf{E}_i$ and additional parameters (which will not be pre-eliminated) and a parameter array $\Delta\tilde{\mathbf{v}}_i$ containing $\Delta\mathbf{v}_i$ and other parameters (which will be pre-eliminated at t_i). The generalization of the formulae related to our second method is of a purely formal character and need not be further discussed here. In essence, we have to keep track of subinterval-dependent parameter arrays (with subinterval-dependent dimensions) $\Delta\tilde{\mathbf{E}}_i$ and $\Delta\tilde{\mathbf{v}}_i$ to be retained and eliminated, respectively, at the end of the subinterval $[t_i, t_{i+1})$, respectively.

Whether or not the resulting algorithm is efficient depends almost uniquely on the dimensions of the arrays $\Delta\tilde{\mathbf{E}}_i$ (the number of parameters not pre-eliminated at the ends of the subintervals).

5.2 The full normal equation system for method 2

It is instructive to look at the full normal equation system when using the parameterization with the osculating elements $\mathbf{E}_{n-1}$ and the pulses $\mathbf{v}_i$, $i = 1, 2, \ldots, n-1$. This system is obtained by applying the parameter transformation specified in Sect. 5.1, but not the pre-elimination at the epochs t_i:

$$\begin{pmatrix} \mathbf{A}^{\mathrm{T}}\mathbf{P}\mathbf{A} & -\left\{\sum_{i=0}^{0}\mathbf{N}_i\right\}\mathbf{B}_1 & \ldots & -\left\{\sum_{i=0}^{n-2}\mathbf{N}_i\right\}\mathbf{B}_{n-1} \\ \ldots & \mathbf{B}_1^{\mathrm{T}}\left\{\sum_{i=0}^{0}\mathbf{N}_i\right\}\mathbf{B}_1 & \ldots & \mathbf{B}_1^{\mathrm{T}}\left\{\sum_{i=0}^{0}\mathbf{N}_i\right\}\mathbf{B}_{n-1} \\ \ldots & \ldots & \ldots & \ldots \\ \ldots & \ldots & \ldots & \ldots \\ \ldots & \ldots & \ldots & \mathbf{B}_{n-1}^{\mathrm{T}}\left\{\sum_{i=0}^{n-2}\mathbf{N}_i\right\}\mathbf{B}_{n-1} \end{pmatrix} \cdot \begin{pmatrix} \Delta\mathbf{E}_{n-1} \\ \Delta\mathbf{v}_1 \\ \Delta\mathbf{v}_2 \\ \ldots \\ \ldots \\ \Delta\mathbf{v}_{n-1} \end{pmatrix} = \begin{pmatrix} \mathbf{A}^{\mathrm{T}}\mathbf{P}\Delta\boldsymbol{\phi} \\ -\mathbf{B}_1^{\mathrm{T}}\sum_{i=0}^{0}\mathbf{A}_i^T\mathbf{P}_i\cdot\Delta\boldsymbol{\phi}_i \\ -\mathbf{B}_2^{\mathrm{T}}\sum_{i=0}^{1}\mathbf{A}_i^T\mathbf{P}_i\cdot\Delta\boldsymbol{\phi}_i \\ \ldots \\ \ldots \\ -\mathbf{B}_{n-1}^{\mathrm{T}}\sum_{i=0}^{n-2}\mathbf{A}_i^T\mathbf{P}_i\cdot\Delta\boldsymbol{\phi}_i \end{pmatrix}, \tag{62}$$

where $\mathbf{N}_i = \mathbf{A}_i^{\mathrm{T}}\mathbf{P}_i\mathbf{A}_i$.

Equation 62 illustrates (once more) that it is indeed possible to pre-eliminate the parameter array $\Delta\mathbf{v}_1$ after having processed the observations in the interval $[t_0, t_1]$, $\Delta\mathbf{v}_2$ after having processed those in the interval $(t_1, t_2]$, etc. Observe that this pre-elimination is only possible thanks to the transformation Eq. 38.

Let us point out that (apart from the definition of the initial osculating elements), Eq. 62 is equivalent to Eq. 25 referring to the original, untransformed orbital elements.

6 Conventional estimation of piecewise constant accelerations

The discontinuities of $\dot{\mathbf{r}}(t)$ encountered at the epochs t_i, $i = 1, 2, \ldots, n-1$, which occur when modelling the orbits with pseudo-stochastic pulses, are disadvantageous for certain applications such as the orbit computation necessary for atmospheric sounding using the GPS occultation method. Therefore, Jäggi et al. (2004) showed how to replace these pulses by piecewise constant accelerations. The arc (the integration interval) is subdivided into n subintervals—exactly like in the case of pseudo-stochastic pulses. One set of (at maximum) three constant accelerations in three pre-determined directions $\mathbf{e}_{ij}(t)$ are set up within each of the subintervals $[t_i, t_{i+1})$, $i = 0, 1, \ldots, n-1$.

The pre-determined directions may be chosen to be time-independent in one coordinate system (e.g. defined by the radial, along-track and out-of-plane directions) and therefore usually time-dependent in the inertial coordinate system. When modelling the orbit with piecewise constant accelerations, the equation of motion reads

$$\ddot{\mathbf{r}} = \mathbf{f}\,(\mathbf{r}, \dot{\mathbf{r}}, t) + \sum_{j=1}^{3} \Delta a_{ij}\ \mathbf{e}_{ij}(t)\ ,$$
$$t \in [t_{i-1}, t_i), \quad i = 1, \ldots n\ . \tag{63}$$

where Δa_{ij} are the unknowns of the parameter estimation process (together with the six initial osculating elements).

The partial derivative of the orbit w.r.t. the parameter Δa_{ij} is governed by the following variational equation:

$$\ddot{\mathbf{z}}_{ij} = \mathbf{A}_0(t)\ \mathbf{z}_{ij} + \mathbf{A}_1(t)\ \dot{\mathbf{z}}_{ij} + \begin{cases} \mathbf{e}_{ij}(t) & t \in [t_{i-1}, t_i) \\ \mathbf{0} & \text{elsewhere} \end{cases}\ , \tag{64}$$

where the 3×3 matrices $\mathbf{A}_i(t)$ are the Jacobian matrices of the deterministic functions $\mathbf{f}(t) \stackrel{\text{def}}{=} \mathbf{f}(\mathbf{r}, \dot{\mathbf{r}}, t)$ (the force per mass unit acting on the satellite) w.r.t. $\mathbf{r}$ and $\dot{\mathbf{r}}$, respectively, and where

$$\mathbf{z}_{ij}(t) \stackrel{\text{def}}{=} \frac{\partial \mathbf{r}_0(t)}{\partial \Delta a_{ij}}\ . \tag{65}$$

The homogeneous part of Eq. 64 is identical to Eq. 7. The functions $\mathbf{z}_{ij}(t)$ meet the following initial conditions (implying continuity of both the position and velocity vectors):

$$\mathbf{z}_{ij}(t_{i-1}) = \dot{\mathbf{z}}_{ij}(t_{i-1}) = \mathbf{0}\ . \tag{66}$$

The initial value problem (Eqs. 64 and 66) is solved by a linear combination of the solutions $\mathbf{z}_k, k = 1, 2, \ldots, 6$ corresponding to the initial osculating elements at t_0. The coefficients of the linear combination are time-dependent within the interval $[t_{i-1}, t_i)$, they are zero for previous intervals, and non-zero, constant and identical for intervals $[t_k, t_{k+1}]$, $k > i - 1$:

$$\mathbf{z}_{ij}(t) \stackrel{\text{def}}{=} \begin{cases} \mathbf{0} & t < t_{i-1} \\ \tilde{\mathbf{z}}_{ij}(t) = \sum_{k=1}^{6} \beta_{ij,k}(t) \cdot \mathbf{z}_k(t) & t \in [t_{i-1}, t_i) \\ \sum_{k=1}^{6} \beta_{ij,k}(t_i) \cdot \mathbf{z}_k(t) \stackrel{\text{def}}{=} \sum_{k=1}^{6} \beta_{ij,k} \cdot \mathbf{z}_k(t) & t \geq t_i \end{cases}\ . \tag{67}$$

The actual computation of the functions $\tilde{\mathbf{z}}_{ij}(t)$ may be found in Jäggi et al. (2004).

Equation 67 should be compared to Eq. 16, which is the equivalent equation, when pulses instead of accelerations are introduced . As opposed to the case of pulses, we have to distinguish three regimes, namely one where the partial derivatives are zero, one where they are a linear combination with time-dependent coefficients of the corresponding six partial derivatives w.r.t. the initial osculating elements and one where they are a linear combination with constant coefficients of the same derivatives.

The constant coefficients of the linear combination in the interval $[t_i\,, t_n]$ are obtained as solutions of the following linear condition equations:

$$\sum_{k=1}^{6} \beta_{ij,k} \cdot \mathbf{z}_k(t_i) = \tilde{\mathbf{z}}_{ij}(t_i)\ ; \quad \sum_{k=1}^{6} \beta_{ij,k} \cdot \dot{\mathbf{z}}_k(t_i) = \dot{\tilde{\mathbf{z}}}_{ij}(t_i), \tag{68}$$

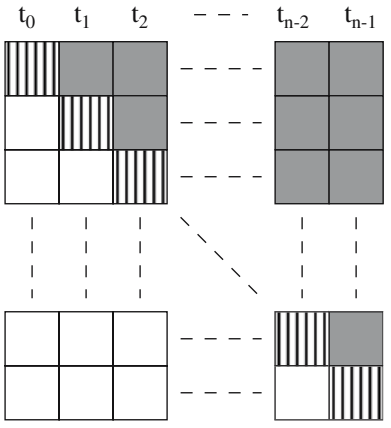

Fig. 2 Activity intervals of piecewise constant accelerations. *Blank zones* partial derivatives w.r.t. parameters are zero, *mixed zones* "|||" partial derivatives are a linear combination of partial derivatives w.r.t. initial elements with time-dependent coefficients, *grey zones* partial derivatives are a linear combination of derivatives w.r.t. initial elements with constant coefficients

which should be compared to Eq. 17, representing the condition equations in the case of pulses.

The relationship between the two sets of condition equations becomes obvious if we approximate the solutions $\tilde{\mathbf{z}}_{ij}(t)$ by a Taylor series up to second order in $t - t_i$:

$$\sum_{k=1}^{6} \beta_{ij,k} \cdot \mathbf{z}_k(t_i) \approx \frac{1}{2}\Delta t^2\ \mathbf{e}_{ij}(t_i) \approx \mathbf{0},$$
$$\sum_{k=1}^{6} \beta_{ij,k} \cdot \dot{\mathbf{z}}_k(t_i) \approx \Delta t\ \mathbf{e}_{ij}(t_i)\ , \tag{69}$$

where $\Delta t = t_{i+1} - t_i$. By comparing Eqs. 17 and 68, we conclude that up to terms of the first order in Δt we have

$$\Delta \mathbf{v}_{ij} = \Delta t\ \Delta \mathbf{a}_{ij}\ . \tag{70}$$

Figure 2 illustrates the three regimes for all stochastic parameters set up. Blank zones indicate time intervals where the partial derivatives w.r.t. the parameter are zero, zones marked with "|||" indicate the time interval where the linear combination has time-dependent coefficients, and grey zones indicate time intervals where the partial derivatives may be represented by a linear combination (of the partial derivatives w.r.t. the initial osculating elements) with constant coefficients. Apart from that, Figs. 1 and 2 are identical. Note that there is one more set of (at most three) constant accelerations than pseudo-stochastic pulses. The number of active (i.e. non-zero) parameters varies from $6 + 3$ in subinterval $[t_0, t_1)$ to $6 + 3n$ in subinterval $[t_{n-1}, t_n]$.

Like in the case of pseudo-stochastic pulses, we observe a roughly linear growth of the number of active parameters with time, implying a quadratic growth in the storage requirements and a cubic growth in processing time.

7 Piecewise constant accelerations: efficient method 1

When modelling the orbit with pseudo-stochastic pulses, the observation equations related to the subinterval $[t_i, t_{i+1})$ could be written in the form of Eq. 23. When modelling the orbit with piecewise constant accelerations, the observation equations read

$$\mathbf{A}_i \cdot \Delta\mathbf{E}_0 + \mathbf{A}_i \cdot \sum_{m=1}^{i} \mathbf{B}_m \cdot \Delta\mathbf{a}_m + \mathbf{A}_{\mathrm{ca},i+1}\Delta\mathbf{a}_{i+1} - \Delta\boldsymbol{\phi}_i = \boldsymbol{\rho}_i \ , \tag{71}$$

where $\mathbf{A}_{\mathrm{ca},i+1}$ is the matrix containing the partial derivatives of the observed functions w.r.t. the constant accelerations pertaining to the current subinterval $[t_i, t_{i+1})$.

It is convenient to use the same designation for the coefficient matrices $\mathbf{B}_i$ for both types of modelling: the pseudo-stochastic pulses and the piecewise constant accelerations. One should, however, keep in mind that the coefficients are defined in a different way (cf. Eqs. 17 and 68).

In Sect. 5 Eqs. 36 and 37, we pointed out that

$$\Delta\mathbf{E}_i \stackrel{\mathrm{def}}{=} \Delta\mathbf{E}_0 + \sum_{m=1}^{i} \mathbf{B}_m \cdot \Delta\mathbf{v}_m \tag{72}$$

represents the set of initial osculating elements solving Eq. 1 in the interval $[t_i, t_{i+1})$. The resulting orbit solves one and the same set of equations of motion in each subinterval but with different initial conditions.

When modelling the orbits with piecewise constant accelerations, the equation of motion is given by Eq. 63. Equation 63 thus changes from subinterval to subinterval and each equation differs from Eq. 1 describing the underlying deterministic problem. It is, however, still possible to define a set of elements characterizing the initial conditions referring to the subinterval $[t_i, t_{i+1})$ by

$$\Delta\mathbf{E}_i \stackrel{\mathrm{def}}{=} \Delta\mathbf{E}_0 + \sum_{m=1}^{i} \mathbf{B}_m \cdot \Delta\mathbf{a}_m, \tag{73}$$

where the elements $\Delta\mathbf{E}_i$, defined by Eq. 73, represent the initial osculating elements (at time t_0) of the particular solution, which solves Eq. 63 in the subinterval $[t_i, t_{i+1})$.

In analogy to Sect. 4, here we analyze the structure of the full normal equation system when parameterizing the orbit with six initial osculating elements and n (not $n-1$) piecewise constant accelerations. Let us define the vector of the unknown parameters as

$$\mathbf{p}_{\mathrm{ca}}^{\mathrm{T}} \stackrel{\mathrm{def}}{=} \left(\Delta\mathbf{E}_0^{\mathrm{T}}, \Delta\mathbf{a}_1^{\mathrm{T}}, \Delta\mathbf{a}_2^{\mathrm{T}}, \ldots, \Delta\mathbf{a}_{n-1}^{\mathrm{T}}, \Delta\mathbf{a}_n^{\mathrm{T}}\right) \ , \tag{74}$$

where $\Delta\mathbf{a}_i$ is the (column) array of three constant accelerations Δa_{ij}, $j = 1, 2, 3$, referring to the subinterval $[t_{i-1}, t_i)$.

Let us write the full normal equation system as

$$\mathbf{N}_{\mathrm{ca}} \cdot \mathbf{p}_{\mathrm{ca}} = \mathbf{b}_{\mathrm{ca}} \ , \tag{75}$$

where the matrices can be written as sums of two terms, the first ones of which are (almost) identical with Eq. 25 obtained in the case of the pseudo-stochastic pulses, and contributions due to the piecewise constant accelerations stemming from the subinterval that they refer to. The matrices in Eq. 75 may thus be written:

$$\mathbf{N}_{\mathrm{ca}} = \mathbf{N}_{\mathrm{ps}} + \Delta\mathbf{N}_{\mathrm{ca}} \ , \quad \mathbf{b}_{\mathrm{ca}} = \mathbf{b}_{\mathrm{ps}} + \Delta\mathbf{b}_{\mathrm{ca}}. \tag{76}$$

The matrix corresponding to the pseudo-stochastic pulses reads

$$\mathbf{N}_{\mathrm{ps}} = \begin{pmatrix} \mathbf{A}^{\mathrm{T}}\mathbf{P}\mathbf{A} & \sum_{i=1}^{n-1} \mathbf{A}_i^{\mathrm{T}}\mathbf{P}_i\mathbf{A}_i\ \mathbf{B}_1 & \cdots \\ \cdots & \left[\mathbf{B}_1^{\mathrm{T}} \sum_{i=1}^{n-1} \mathbf{A}_i^{\mathrm{T}}\mathbf{P}_i\mathbf{A}_i\ \mathbf{B}_1\right]' & \cdots \\ \cdots & \cdots & \cdots \\ \cdots & \cdots & \cdots \\ \cdots & \cdots & \cdots \\ \mathbf{0} & \mathbf{0} & \mathbf{0} \end{pmatrix}$$

$$\begin{pmatrix} \sum_{i=n-1}^{n-1} \mathbf{A}_i^{\mathrm{T}}\mathbf{P}_i\mathbf{A}_i\ \mathbf{B}_{n-1} & \mathbf{0} \\ \mathbf{B}_1^{\mathrm{T}} \sum_{i=n-1}^{n-1} \mathbf{A}_i^{\mathrm{T}}\mathbf{P}_i\mathbf{A}_i\ \mathbf{B}_{n-1} & \mathbf{0} \\ \cdots & \cdots \\ \cdots & \cdots \\ \left[\mathbf{B}_{n-1}^{\mathrm{T}} \sum_{i=n-1}^{n-1} \mathbf{A}_i^{\mathrm{T}}\mathbf{P}_i\mathbf{A}_i\ \mathbf{B}_{n-1}\right]' & \mathbf{0} \\ \mathbf{0} & \mathbf{W} \end{pmatrix}, \tag{77}$$

and the corresponding matrix on the right-hand side of Eq. (76) is

$$\mathbf{b}_{\mathrm{ps}} = \begin{pmatrix} \mathbf{A}^{\mathrm{T}}\mathbf{P}\Delta\boldsymbol{\phi} \\ \mathbf{B}_1^{\mathrm{T}} \sum_{i=1}^{n-1} \mathbf{A}_i^{\mathrm{T}}\mathbf{P}_i \cdot \Delta\boldsymbol{\phi}_i \\ \mathbf{B}_2^{\mathrm{T}} \sum_{i=2}^{n-1} \mathbf{A}_i^{\mathrm{T}}\mathbf{P}_i \cdot \Delta\boldsymbol{\phi}_i \\ \cdots \\ \cdots \\ \mathbf{B}_{n-1}^{\mathrm{T}} \sum_{i=n-1}^{n-1} \mathbf{A}_i^{\mathrm{T}}\mathbf{P}_i \cdot \Delta\boldsymbol{\phi}_i \\ \mathbf{0} \end{pmatrix} . \tag{78}$$

The matrices in Eq. 77 are identical to the corresponding matrices in Eq. 25 for the model based on pulses (after having added the constraints; see Eq. 28, except for the last line (and column), which corresponds to the acceleration $\Delta\mathbf{a}_n$ of the last subinterval $[t_{n-1}, t_n]$)

The terms that are due to the piecewise constant accelerations in their subintervals read

$$\Delta\mathbf{N}_{\mathrm{ca}} = \begin{pmatrix} \mathbf{0} & \mathbf{A}_0^{\mathrm{T}}\mathbf{P}_0\mathbf{A}_{\mathrm{ca},0} & \cdots \\ \cdots & \mathbf{A}_{\mathrm{ca},0}^{\mathrm{T}}\mathbf{P}_0\mathbf{A}_{\mathrm{ca},0} & \cdots \\ \cdots & \cdots & \cdots \\ \cdots & \cdots & \cdots \\ \cdots & \cdots & \cdots \\ \cdots & \cdots & \cdots \end{pmatrix}$$

$$\begin{pmatrix} \mathbf{A}_{n-2}^{\mathrm{T}}\mathbf{P}_{n-2}\mathbf{A}_{\mathrm{ca},n-2} & \mathbf{A}_{n-1}^{\mathrm{T}}\mathbf{P}_{n-1}\mathbf{A}_{\mathrm{ca},n-1} \\ \mathbf{B}_1^{\mathrm{T}}\mathbf{A}_{n-2}^{\mathrm{T}}\mathbf{P}_{n-2}\mathbf{A}_{\mathrm{ca},n-2} & \mathbf{B}_1^{\mathrm{T}}\mathbf{A}_{n-1}^{\mathrm{T}}\mathbf{P}_{n-1}\mathbf{A}_{\mathrm{ca},n-1} \\ \cdots & \cdots \\ \cdots & \cdots \\ \mathbf{A}_{\mathrm{ca},n-2}^{\mathrm{T}}\mathbf{P}_{n-2}\mathbf{A}_{\mathrm{ca},n-2} & \mathbf{B}_{n-1}^{\mathrm{T}}\mathbf{A}_{n-1}^{\mathrm{T}}\mathbf{P}_{n-1}\mathbf{A}_{\mathrm{ca},n-1} \\ \cdots & \mathbf{A}_{\mathrm{ca},n-1}^{\mathrm{T}}\mathbf{P}_{n-1}\mathbf{A}_{\mathrm{ca},n-1} \end{pmatrix} \tag{79}$$

and

$$\Delta\mathbf{b}_{ca} = \begin{pmatrix} \mathbf{0} \\ \mathbf{A}_{\mathrm{ca},0}^{\mathrm{T}}\mathbf{P}_0 \cdot \boldsymbol{\Delta\phi}_0 \\ \mathbf{A}_{\mathrm{ca},1}^{\mathrm{T}}\mathbf{P}_1 \cdot \boldsymbol{\Delta\phi}_1 \\ \cdots \\ \cdots \\ \mathbf{A}_{\mathrm{ca},n-1}^{\mathrm{T}}\mathbf{P}_{n-1} \cdot \boldsymbol{\Delta\phi}_{n-1} \end{pmatrix} . \tag{80}$$

We are now in a position to set up the full normal equation system in a very efficient way. From the algorithms' point of view, the differences w.r.t. the case of pseudo-stochastic pulses are marginal (at least from the point of view of computational efficiency). These differences may be summarized as

- When setting up the normal equation contribution in the subinterval $[t_i, t_{i+1})$, we have to take into account the partial derivatives w.r.t. $\Delta\mathbf{a}_{i+1}$. This means that these contributions are described by matrices of dimension $d = 6 + 3 = 9$ and not $d = 6$ as in the case of pseudo-stochastic pulses.
- The coefficient matrices $\mathbf{B}_i$ are defined in a slightly different way (cf. Eqs. 17 and 68).
- When setting up the full normal equation system, we have to add the contributions $\Delta\mathbf{N}_{\mathrm{ca}}$ and $\Delta\mathbf{b}_{\mathrm{ca}}$ (see Eqs. 79 and 80) to the matrices $\mathbf{N}_{\mathrm{ps}}$ and $\mathbf{b}_{\mathrm{ps}}$ (see Eqs. 77 and 78).

8 Piecewise constant accelerations: efficient method 2

In view of the developments outlined in Sect. 7, it is clear that the algorithm corresponding to our second method (Sect. 5) may also be established easily. In essence, we have to modify Eqs. 44 in order to take into account that the accelerations of subinterval i are present when setting up the normal equation contribution of interval i. After having added the weights, the pre-elimination step may take place in the same way as in the case of the pseudo-stochastic pulses.

When calculating the variance–covariance matrix associated with the position vector $\mathbf{r}(t)$ for $t \in [t_i, t_{i+1})$, one has to take into account that the orbit de facto is a function of the set of elements $\Delta\mathbf{E}_i$ and the accelerations $\Delta\mathbf{a}_{i+1}$:

$$\mathbf{r}(t) = \mathbf{r}_0(t) + \sum_{k=1}^{6} \frac{\partial\mathbf{r}_0(t)}{\partial E_k^i} \cdot \Delta E_k^i + \sum_{j=1}^{3} \frac{\partial\mathbf{r}_0(t)}{\partial\Delta a_{i+1,j}} \cdot \Delta a_{i+1,j} \, . \tag{81}$$

This is why the variance–covariance matrix (Eq. 57) associated with $\Delta\mathbf{E}_i$ and $\Delta\mathbf{a}_{i+1}$ is needed to calculate the variance–covariance matrix associated with $\mathbf{r}(t)$. The orbit is thus defined in each subinterval by nine parameters in the case of piecewise constant accelerations (as opposed to six in the case of pseudo-stochastic pulses). A similar statement holds for the velocity vector $\dot{\mathbf{r}}(t)$ or for any function $f(\mathbf{r}(t), \dot{\mathbf{r}}(t))$.

9 Piecewise linear accelerations

When modelling an orbit with piecewise constant accelerations, one has the "problem" of discontinuities in the second derivatives of the position vector: the accelerations are discontinuous at the subinterval boundaries. There is, however, no physical reason for such discontinuities. This is why Jäggi et al. (2006) studied orbit modelling with piecewise linear (and continuous) accelerations. By introducing this model, the discontinuity problem is (again) transferred to the next higher derivative (they do now occur on the level of the first derivatives of the accelerations).

One might first think that the number of pseudo-stochastic parameters would be doubled when replacing the piecewise constant by the piecewise linear accelerations because we have to model the acceleration within each subinterval by a straight line (polynomial of degree one with two adjustable parameters). By enforcing continuity at the subinterval boundaries, the number of independent parameters is, however, reduced to roughly the same number as in the case of piecewise constant accelerations. The "trick" resides in the fact that the values of the accelerations at the subinterval boundaries are introduced as the unknown parameters of the orbit determination process (and not one offset and one drift per interval).

According to Jäggi et al. (2006), the acceleration in a particular direction $\mathbf{e}(t)$ in a particular subinterval is modelled by

$$\Delta\mathbf{a}(t) = \frac{t - t_{i-1}}{t_i - t_{i-1}} \cdot \Delta a_i \cdot \mathbf{e}(t) + \frac{t_i - t}{t_i - t_{i-1}} \cdot \Delta a_{i-1} \cdot \mathbf{e}(t), \tag{82}$$

which automatically enforces continuity at the subinterval boundaries. The variational equation for parameter Δa_i, $i \neq 0$ and $i \neq n-1$ reads

$$\ddot{\mathbf{z}}_{a_i} = \mathbf{A}_0 \cdot \mathbf{z}_{a_i} + \begin{cases} \left(\frac{t - t_{i-1}}{\Delta_{i,i-1}}\right)\mathbf{e}(t) & t_{i-1} \leq t < t_i \\ \left(\frac{t_{i+1} - t}{\Delta_{i+1,i}}\right)\mathbf{e}(t) & t_i \leq t < t_{i+1} \\ \mathbf{0} & \text{else} \end{cases} , \tag{83}$$

where $\Delta_{i,j} \doteq t_i - t_j$. For $i = 0$ and $i = n - 1$ Eq. 83 is even simpler, because the first or second of the above cases of the inhomogeneous part of Eq. 83 do not occur, respectively.

The unknowns of the orbit determination process are Δa_i, $i = 0, 1, \ldots, n$. A correct count of the unknowns reveals that we only have one more set of (at most three) unknowns than in the case of piecewise constant acceleration.

An inspection of Eq. 83 shows that accelerations of the type $\sim t \cdot \mathbf{e}$ (i.e. proportional to time t) occur in its inhomogeneous part. This implies that we need the solution of the six variational equations for the six initial osculating elements, the three constant accelerations in the three orthogonal directions and three linearly growing accelerations in the same three orthogonal directions, in order to calculate all the required partial derivatives. The partial derivatives w.r.t. all Δa_i may thus be computed as a linear combination of the mentioned $6 + 3 + 3 = 12$ solutions of the variational equations. For details, we refer to Jäggi et al. (2006).

From this point onwards, (the classic and) efficient solution of the orbit determination problem follows the same pattern as that explained in Sect. 8. The differences (although at times tricky in the fine detail of implementation) are minor in nature and can be summarized as follows:

- There are two sets of accelerations, those referring to the left and the right subinterval boundaries, active in each subinterval (there is only one set active in the case of piecewise constant accelerations, and none in the case of pulses).
- The set of accelerations referring to the left interval boundary may be pre-eliminated after having added the last contribution to the normal equation system of the current subinterval.
- For the pre-elimination and the back-substitution processes, the set of accelerations referring to the left interval boundary formally has to be considered as "normal" orbit parameters in the current subinterval.

Having shown that the cases of piecewise constant and piecewise linear accelerations are very closely related and having pointed out the "major" differences (which are actually minor in nature), we will not further discuss the case of piecewise linear accelerations in this article, which focuses on the mathematical structure of the algorithms and on their efficiency.

Let us point out that the achievable quality of orbits parameterized with the three orbit models is a different issue. We refer to Jäggi et al. (2006) for more information.

10 Tests with CHAMP and ground-based GPS observations

10.1 Overview

The algorithms outlined above have been implemented into a development version of the Bernese GPS software, Version 5.1, (Hugentobler et al. 2005). This version allows it to generate kinematic orbits (estimating one LEO position per observation epoch) using code and/or carrier-phase zero and/or double-difference observations, as well as reduced-dynamic orbits, by setting up pseudo-stochastic parameters in the classical way (see Sect. 3). Major parts were developed in close cooperation with the Technical University of Munich (e.g. Švehla and Rothacher 2002, 2003). Our developments are almost entirely contained in one Fortran90 module consisting of four subroutines.

One entire day of CHAMP data (day 198 of year 2002, corresponding to July 17, 2002) is subsequently analyzed, where we only focus on the efficiency of the parameter estimation processes. The ionosphere-free linear combination of the carrier-phase observations was used. The results of the CODE analysis center (Hugentobler et al. 2003) of the International GNSS Service (IGS) (Dow et al. 2005) were used to perform the following three tests:

1. *Analysis of CHAMP zero-difference code observations*. This example corresponds very closely to the theory presented above, as there are "only" six deterministic orbit parameters and the pseudo-stochastic parameters involved in the analysis.
2. *Analysis of CHAMP zero-difference carrier-phase observations*. The example asks for a more general than the usual "filter-type" environment, because the carrier-phase ambiguity parameters also have to be taken into account.
3. *Analysis of double-difference carrier-phase observations of a large network of ground-based GPS receivers and the spaceborne CHAMP receiver.* This is the most ambitious of the tests performed, as there is a large number (thousands) of ambiguity parameters involved. The results of the CODE analysis center (coordinates of the ground network, troposphere parameters) were extensively used in this case.

The tests were performed on an HP Compac nc6000 Business Notebook with a 1.60 GHz processor. The program runs were performed in a DOS-window of an XP professional Microsoft Windows environment. The RAM available during runtime was limited to about 1.5 Gbytes.

10.2 Analysis of the LEO zero difference code observations

Code observations with a spacing of 30s on both the L1 and the L2 carriers to all GPS satellites in view, gathered by the LEO spaceborne GPS receiver, are available and were analyzed in the test runs below. The ionosphere-free linear combination L_3 was formed from the original L_1 and L_2 observations (Teunissen and Kleusberg 1998). A total of about 22,500 L_3 code zero-difference observations were accumulated by the CHAMP receiver on day 198 of year 2002. The following tests were performed each at 15, 12, 10, 8, 6, 5, 4, 3, 2, 1 and 0.5 min intervals:

- The classical method (not making use of any of the efficient methods) was applied to the case of pseudo-stochastic pulses.

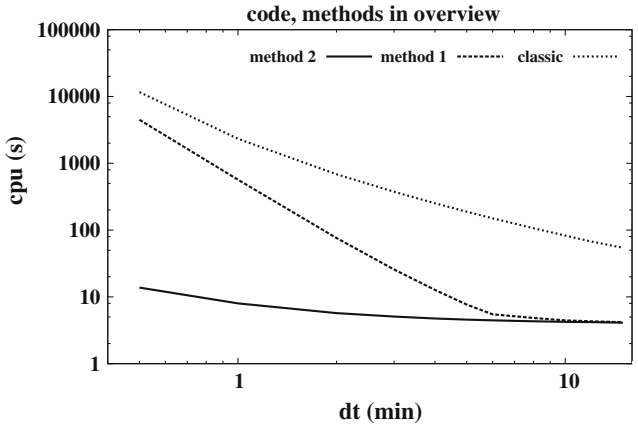

Fig. 3 CPU times for classical, filter methods 1 and 2. Code zero-difference processing with pseudo-stochastic pulses

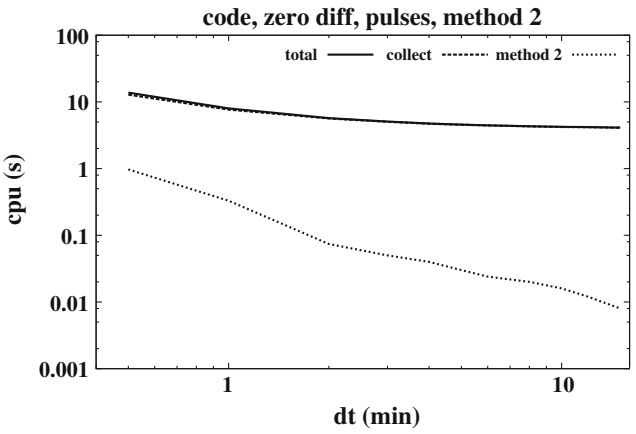

Fig. 4 CPU times for data collection, pre-elimination and updating. Analysis for 1 day of CHAMP data using method 2 with pseudo-stochastic pulses

– Method 1 (setting up the normal equation system in an efficient way, but inverting the full matrix) was applied to the case of pseudo-stochastic pulses.
– Method 2 (using the pre-elimination, back-substitution approach) was applied to the case of pseudo-stochastic pulses and to the case of accelerations.

As a day contains 1,440 min, the total number of parameters varies between $6 + 95 \times 3 = 291$ for 15 min intervals (pseudo- stochastic pulses) and $6 + 2,880 \times 3 = 8,646$ for 30 sec intervals (piecewise constant accelerations). As a consequence, the computation (CPU) times varies by orders of magnitude with the length of the subintervals.

Figure 3 shows the total processing time (CPU time in seconds) as a function of the subinterval length (which is also indirectly proportional to the number of pulses) when setting up pseudo-stochastic pulses. It takes 8s, 9 min 28s, and 38 min 48s of CPU time to process the entire day of code data when using method 2, method 1 and the classical method, respectively, when selecting a subinterval length of 1 min. Obviously, method 2 is orders of magnitude more efficient than the other two methods.

It is, however, remarkable that method 1, down to a subinterval length of 1 min is still feasible: a processing time of less than 10 minutes (for a 1 min spacing between pulses) may be acceptable, even in a routine computational environment. The gain w.r.t. the classical method is a factor of about four. If the full variance–covariance matrix is required, method 1 is the best one available. Obviously, the classical approach cannot be recommended in view of the efficiency of the former two methods.

The growth of the CPU time as a function of the subinterval length differs substantially for the three methods (Fig. 3). The processing time for method 1 is dominated by the time it takes to invert the normal equation matrix for the subinterval length $\Delta t \to 0$. Matrix inversion algorithms are proportional to the cube of the dimension of the matrix (Press et al. 1996). It seems that the asymptotic behaviour of the CPU time for $\Delta t \to 0$ is "only" roughly proportional to Δt^2 in the case of the classical method.

This is, however, not correct, because the growth seen in Fig. 3 is still dominated by the process of setting up the normal equation system and not by the matrix inversion. The asymptotic behaviour for the classical method must also contain the Δt^3-term for $\Delta t \to 0$. The curves for the two methods (classical and method 1) must become tangential, asymptotically. It would, however, cost hours of CPU to "prove" this statement.

Let us now analyze in more detail the processing time for the two efficient methods 1 and 2. In Fig. 4, the CPU required to read the data and set up the normal equation systems for each time interval (this part of the required CPU is referred to as "collect" in Fig. 4) is distinguished from the CPU required by method 2, assuming that the normal equation systems are available.

Figure 4 thus reveals that in the case of method 2, the total CPU time (solid line) is almost entirely caused by the process of setting up the normal equation contributions for the subintervals (starting from the observation equations, resulting in the normal equation contribution). The pre-elimination and the back-substitution steps are almost "free of charge" compared to the data collection part. For very long data spans (several days and/or very high sampling rates), the algorithm's CPU requirements would eventually become dominant w.r.t. to the CPU required by the collection part.

Figure 5 shows that in the case of method 1, the processing time is dominated by the inversion of the full normal equation system (term proportional to Δt^3). The processing times become prohibitively long for the shortest subinterval lengths.

The algorithms based on piecewise constant accelerations are slightly less efficient than those based on pulses (see Fig. 6 and compare it with Fig. 4). The slight growth of processing time is caused by the fact that the contributions to the full normal equation system referring to a particular subinterval contain one set of stochastic orbit parameters (instead of none in the case of pulses). Also, the partial derivatives

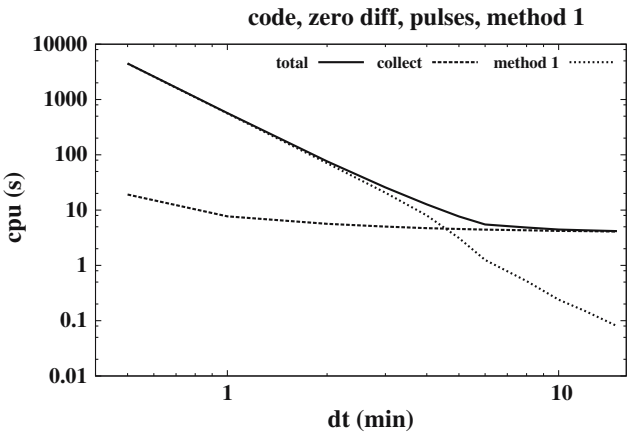

Fig. 5 CPU times for data collection, pre-elimination and updating. Analysis for 1 day of CHAMP data using method 1 with pseudo-stochastic pulses

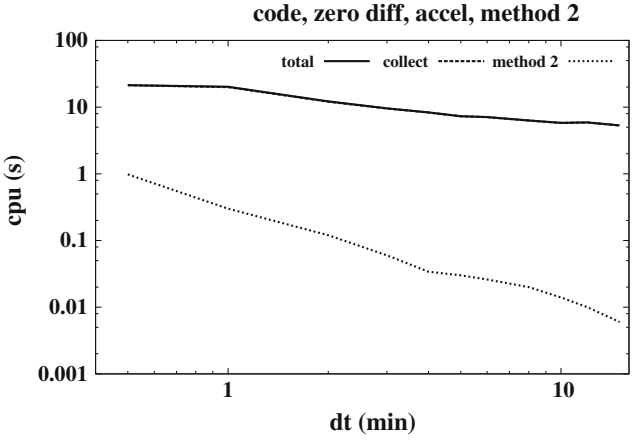

Fig. 6 CPU times for data collection, pre-elimination and updating. Analysis for 1 day of CHAMP data using method 2 with piecewise constant accelerations

w.r.t. the stochastic parameters set up at the beginning of the subinterval have to be calculated for each observation.

The additional amount of work caused by selecting piecewise constant (or piecewise linear) accelerations (and not pulses) to account for the stochastic part of the orbit merely costs a few seconds of additional CPU in that part of the algorithm dealing with the set up of the normal equation system in the subintervals.

Jäggi et al. (2006) studied the performance of the algorithms for applications related to gravity field determination. There, the methods based on accelerations gave more accurate results. For other applications, methods based on pulses, however, may be preferable. As accuracy issues are not central here and as the differences in efficiency for the methods based on pulses and accelerations are marginal, we confine ourselves to the documentation of the tests based on pulses from now on.

10.3 Analysis of the LEO zero-difference carrier-phase observations

The tests performed here are the same as to those performed in Sect. 10.2, except that we do now process zero-difference carrier-phase observations. The time-series of carrier-phase observations gathered by the LEO receiver for one particular GPS satellite contains, in addition to the pseudo-range, an unknown additional constant of initial phase ambiguity parameter (Teunissen and Kleusberg 1998). The observable is also referred to as biased pseudo-range. The parameter is the same for all observation epochs, as long as the GPS satellite is above the horizon of the receiving antenna, phase lock is maintained, and cycle slips do not occur.

For ground-based geodetic observations, the number of ambiguity parameters is usually small because the GPS satellites stay for several hours above the horizon of a stationary GPS receiver. The situation is different for a spaceborne GPS receiver: in general, one and the same GPS satellite will be visible only for a few (let us say between 20 and 40) minutes for the LEO antenna due to the rapid change of the observation geometry caused by the LEO orbital motion.

On day 198 of the year 2002, 475 initial phase ambiguity parameters had to be set up. This means that in addition to the initial osculating elements and the stochastic parameters, we also have to solve for the ambiguity parameters.

The efficiency of the algorithms must decrease (compared to the analysis of code observations) due to the additional 475 unknowns. The loss is not dramatic, however, because only a much smaller number of ambiguities (depending on the length of the subintervals) actually are present in a particular subinterval (because the number of simultaneously visible GPS satellites is limited by the number of channels of the LEO GPS receiver). In the case of the Blackjack receiver onboard the CHAMP satellite (and the software release used at the time the observations were made), "only" ten GPS satellites could be tracked simultaneously.

In order to get an overview of the performance of the new and classical algorithms, we performed the same program runs as in Sect. 10.2: for subinterval lengths ranging between 0.5 and 15 min, methods 1 and 2, as well as the classical method, were applied to the set of carrier-phase observations. More than 20, 000 zero-difference carrier-phase observations were processed in every program run. In addition to the three types of program runs mentioned (and already performed in Sect. 10.2), a fourth type of analysis was performed: the implementation allows for method 2 to keep the ambiguity parameters in the analysis, i.e. not to pre-eliminate them as soon as they no longer show up in the normal equation contributions of the subintervals. Figure 7 compares the performance of these four kinds of analysis.

The program runs were performed with pseudo-stochastic pulses to account for the stochastic properties of the orbit. Comparing the results in Fig. 7 with those in Fig. 3, we see that the presence of ambiguity parameters only has a minor impact on the performance. For subintervals of 1 min, a classical run now takes 40 min instead of 38 min; method 1 takes

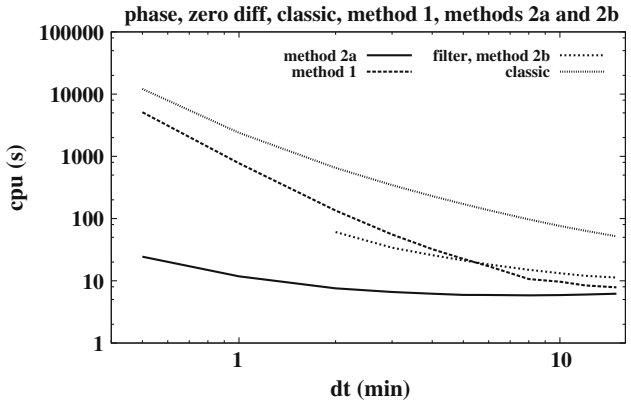

Fig. 7 CPU times for classical, method 1, and filter method 2 with and without ambiguity pre-elimination. Carrier-phase zero-difference processing with pseudo-stochastic pulses

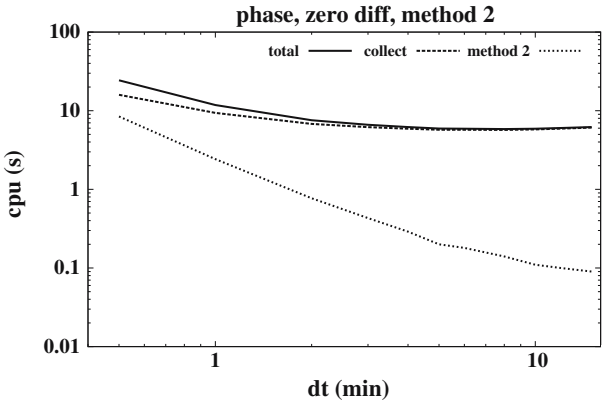

Fig. 8 CPU times for data collection, algorithm (method 2) and total. Carrier-phase zero-difference processing with pseudo-stochastic pulses

13 min instead of 9 min; and method 2 (with pre-elimination of ambiguities) takes 12 s instead of 8 s.

In less than 15 s of CPU time with method 2, one may perform a correct, least-squares, reduced-dynamic LEO solution for a subinterval length of 1 min with about 4, 800 parameters (six initial osculating elements, 475 ambiguities and about $3 \times 1,440 = 4,320$ pseudo-stochastic parameters). Compare this to the 40 min needed for the classical method. The only drawback is that the full variance-covariance matrix is not available with method 2. (The mean errors of all parameters are, however, available and the covariance matrices of satellite positions, velocities, accelerations, etc. may be calculated correctly for each epoch.)

Should the full variance–covariance matrix need to be analyzed, method 1 has to be selected, which, for 1 min subintervals, establishes the solution within about 13 min. For test purposes, it is important to have this option available. Observe, however, that method 1 becomes increasingly inefficient as the number of subintervals (and thus the number of stochastic parameters) grows.

Let us briefly comment on the fourth of the curves contained in Fig. 7, i.e. the results for method 2 without pre-eliminating the 475 ambiguities. There is no justification for selecting this option when processing zero-difference carrier-phase observations. When processing the double-difference carrier-phase observations of LEOs flying in formation (e.g. like GRACE A and B), one has roughly the same number of ambiguity parameters. With this program option, it is possible to resolve the ambiguities in a very efficient way after the update and before the back-substitution step using the full covariance matrix of all the ambiguities and the (few) orbit parameters of the last subinterval.

This method is, as expected, much less efficient than the conventional method 2, but still much more efficient than both the classical method and method 1. It requires much larger storage arrays because dimensions of the intermediary normal equation systems of the subintervals grow to almost 500. This is the solution with a subinterval length of $\Delta t = 1$ min; 30 s was not computed for this method. Note that method 2 without ambiguity pre-elimination requires more CPU than method 1, if only few subintervals are set up, but becomes more efficient with larger numbers of subintervals. The break-even point is reached at about a subinterval length of 6 min.

The distribution of the processing times in the case of the most efficient method (method 2 with pre-elimination of ambiguities) is shown in Fig. 8 and should be compared to Fig. 4, which contains the corresponding information when processing code observations. As in the case of code observations, the total processing time is almost uniquely caused by the data collection part. Only for very long data spans and/or very small subinterval lengths, the time spent in the update and back-substitution steps starts to become important.

10.4 Analysis of the LEO double-difference carrier-phase observations

The CHAMP observations of the same day 198 of 2002 were also analyzed by including them into a double-difference solution using a network of 30, 50 and 70 stationary receivers of the IGS global network. Here, each double difference involves two observations of GPS satellites gathered by the LEO receiver and one ground-based receiver.

The coordinates of the ground-based receivers, troposphere parameters and polar motion were assumed as known in our analysis. This information was taken from the routine analysis of the CODE analysis center of day 198 of year 2002. Consequently, only three parameter types have to be considered, namely deterministic orbit parameters, ambiguity parameters (on the double-difference level) and pseudo-stochastic orbit parameters. Therefore, the mathematical structure of the problem is closely related to that of Sect. 10.3. The main difference resides in the number of ambiguities. This number was 3, 630 in the case of the 30-station network, 6, 422 in the case of the 50-station network and 8, 998 in the case of the 70-station network. The number of

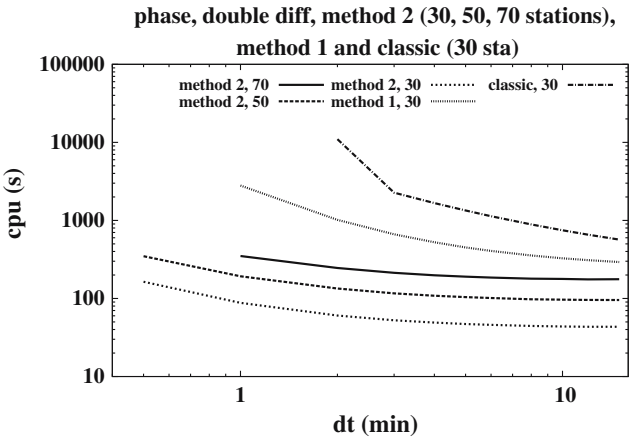

Fig. 9 CPU times for carrier-phase double difference processing of CHAMP data together with a global ground network of 70, 50, and 30 GPS stations for methods 1 and 2 and the classical method with pseudo-stochastic pulses

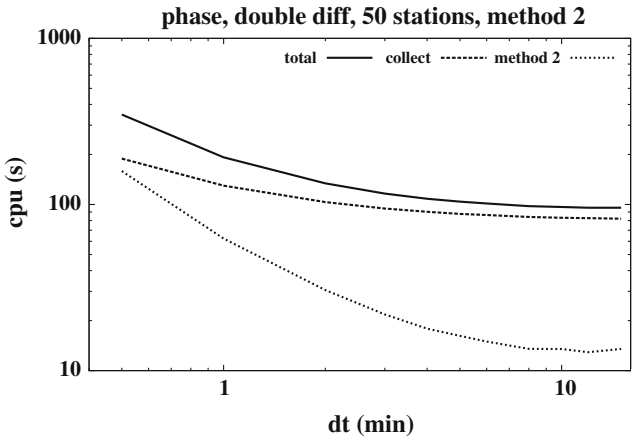

Fig. 11 CPU times for carrier-phase double-difference processing of CHAMP data together with a global network of 50 ground stations: time spent in data collection, algorithm (method 2), total, pseudo-stochastic pulses

double-difference observations was about 115, 000 in the first, 200, 000 in the second and 280, 000 in the third case.

Figure 9 illustrates that the algorithms are still efficient, in particular the algorithm underlying method 2: the solution with 30, 50 and 70 ground stations is obtained within 88 s, 192 s, and 350 s, respectively, when selecting a subinterval length of 1 min and using the same computer.

From Fig. 9, method 1 is much less efficient than method 2, but still much more efficient than the classical method. It takes about 47 min of CPU to generate the solution with subinterval lengths of 1 min with method 1 (for the 30-station ground network). It would probably take more than 10 h to generate the same solution with the classical method. Therefore both the classical method and method 1 are not good candidates for producing reduced-dynamic LEO solutions with a high time resolution on a routine basis. Method 1 remains an excellent choice for test purposes though.

Figure 10, showing the dimension of the normal equation systems for each subinterval resulting in the update (and therefore also in the back-substitution) step for method 2 (70 sites with pre-elimination of ambiguities), indicates why the method is highly efficient: whereas there are close to 9, 000 ambiguities in the full normal equation system, there are hardly ever more than 300 ambiguities to be handled in the subintervals.

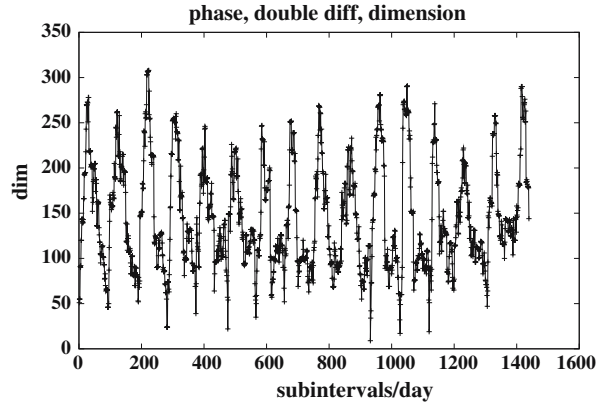

Fig. 10 Dimension of normal equation systems in subintervals of 1 min length (method 2, pre-elimination of ambiguities, ground network of 70 stations, pseudo-stochastic pulses)

This fact does not only reduce the processing time, but also the storage requirements. A double-difference network solution including 100–150 ground stations should be feasible even in a routine computing environment. In the case of the GRACE satellites, it would also be possible to include the space-baseline (between GRACE A and B) with resolved ambiguities into the network solution.

Note that the periodicity of the dimension in Fig. 10 is mainly a consequence of the inhomogeneous ground network. Large dimensions occur if the satellite is flying over regions with many receivers (e.g. over Europe) and small dimensions if the satellite is flying over regions with few receivers (e.g. over large oceans).

Figure 11 is the analogue to Figs. 4 and 8 when processing the double-difference carrier-phase observations from the spaceborne receiver and 50 ground-based receivers. Up to about 5, 000 subintervals the data collection part dominates the processing part if method 2 is used. Only for very long data spans (several days) or a very small subinterval length (few seconds), the time spent in the algorithm part would become important.

11 Summary and outlook

This article is devoted to the development of efficient algorithms for determining the orbits of LEOs in poorly known force fields. The deficiencies of the force field are absorbed either by pseudo-stochastic pulses, piecewise constant accelerations or piecewise linear and continuous accelerations. The normal or "classical" way to deal with these parameters was developed in Sect. 3. The key problem arising is the

growing number of active parameters (see Figs. 1, 2), which leads to very inefficient computations.

It was then shown (Sects. 4 and 5) that the full normal equation system may be set up in a very efficient way, just by making use of the fact that the partial derivatives w.r.t. the orbit parameters may be written as linear combinations of the partial derivatives w.r.t. the initial orbital elements. Some additional terms could be easily accounted for in the case of the piecewise constant and piecewise linear accelerations. The resulting algorithms, called here method 1, still have to invert the full normal equation matrix. Although we showed in Sect. 10 that method 1 is much more efficient than the classical method, it must become inefficient if many stochastic parameters are set up because the time to invert a matrix of dimension d grows proportionally to d^3. Method 1 has, on the other hand, the advantage of making available the full variance–covariance matrix associated with all parameters (deterministic and stochastic orbit parameters, additional parameters).

Method 2 is by far the most efficient of the methods developed here, at least if the number of stochastic parameters is large. It makes use of the parameter transformation (Eq. 38), which associates one set $\mathbf{E}_i$ of initial osculating elements with each subinterval i. If piecewise constant accelerations are used, the orbit within subinterval $[t_i, t_{i+1})$ may be parameterized by the subinterval-specific of elements $\mathbf{E}_i$ and the corresponding acceleration $\Delta\mathbf{a}_{i+1}$ (see Eq. 81). If piecewise linear accelerations are used, the orbit is parameterized within the same subinterval by $\mathbf{E}_i$ and the two accelerations $\Delta\mathbf{a}_i$ and $\Delta\mathbf{a}_{i+1}$.

The processing times associated with method 2 are reduced by about two orders of magnitude when compared to the classical method, by about one order of magnitude when compared to method 1 provided the number of stochastic parameters is of the order of a few thousand. Method 2 therefore is an excellent candidate for high-accuracy orbit modelling in an operational environment. The only disadvantage of method 2 (w.r.t. to the two alternatives) is the fact that the full variance–covariance matrix is not available. The variance–covariance matrix of the parameters active in one particular subinterval is, however, available. This implies (for the three modelling types) that the variance–covariance matrix for the position-, velocity-, acceleration-, etc. vectors at any time t within the arc considered may be easily calculated as well.

The algorithms associated with method 2 resemble a conventional Bayesian filter. If the subinterval length is equal to the data sampling interval, the results—not necessarily the associated variances—become identical. Our method is, however, more general because data sampling and the subinterval length associated with the stochastic parameterization are clearly separated (and may in particular be different) and because other non-orbit parameters may be easily and efficiently incorporated. Also, all parameters have a clear physical definition allowing it, e.g. to calculate the orbit and its derivatives for any time argument.

The introduction of a priori information for the pseudo-stochastic parameters follows the pattern well known in least-squares adjustment, i.e. by introducing artificial observations in connection with a weight matrix. In this article, we uniquely dealt with so-called absolute constraints, i.e. the pseudo-stochastic parameters were constrained w.r.t. the best-fitting (resulting) deterministic orbits. More elaborate statistical information (which would, e.g. constrain the pseudo-stochastic parameters relative to each other) might be introduced, as well, at the price of a slightly more complicated pre-elimination scheme.

Our introduction of pseudo-stochastic orbit parameters avoids the introduction of the concept of stochastic differential equations: the three parameterizations model the orbit in each subinterval as an ordinary differential equation. This is the equation of motion (Eq. 1) reflecting the a priori force field in the case of pseudo-stochastic pulses. It is Eq. 63 that contains one additional (vectorial) term (constant acceleration within the subinterval), in the case of piece-wise constant accelerations.

The solution vector and the statistical information associated with it are the same for all methods outlined above. They correspond to the correct least squares solution of the problem. In addition to the actual (or real) GPS observations, we introduce artificial observations (or pseudo-observations) of the type $\Delta\mathbf{v}_i = \mathbf{0}$ with a user-defined weight matrix $\mathbf{W}$ associated with the parameters $\Delta\mathbf{v}_i$ (the same procedure holds for the accelerations). We treat these as "artificial" observations: They are contained in our observations' statistics and are taken into account for the calculation of the RMS of the weight unit.

The values and the statistical properties of the resulting parameters can therefore be interpreted in the framework of the least-squares theory. The selection of $\mathbf{W}$ is of course critical. Symbolically speaking, we obtain the solution without pseudo-stochastic orbit properties for $\mathbf{W} \to \infty$, we obtain a solution very closely related to the kinematic solution for $\mathbf{W} \to \mathbf{0}$ and if the length of the subintervals equals the spacing between the observations.

We might have added, as a reference, the processing times for kinematic methods. These methods are based on precise point positioning (PPP) using code and/or phase observations and completely disregard the force field, which is known at least approximately. For the technicalities of the PPP method, see Zumberge et al. (1997). Kinematic methods provide no estimate of satellite velocities. Velocities, if calculated at all, have to be established a posteriori by fitting a series of satellite positions by some base functions when using kinematic methods. Let us mention, however, that our method 2 is almost of the same efficiency as the kinematic method when analysing zero difference GPS observations, it is much more efficient than the kinematic case when analysing the double-difference observations gathered by LEOs and a large ground tracking network of GPS receivers.

Acknowledgments We acknowledge with gratitude that this work was in part sponsored by the Swiss National Science Foundation (SNF) under Grant no. 200020-105433.

References

Beutler G (2005) Methods of celestial mechanics. Springer, Berlin Heidelberg New York

Beutler G, Brockmann E, Gurtner W, Hugentobler U, Mervart L, Rothacher M, Verdun A (1994) Extended orbit modeling techniques at the CODE processing center of the international GPS service for geodynamics (IGS): theory and initial results. Manuscr Geod 19:367–386

Colombo OL (1989) The dynamics of global positioning orbits and the determination of precise ephemerides. J Geophys Res 94(B7):9167–9182

Dow JM, Neilan RE, Gendt G (2005) The international GPS service: Celebrating the 10th anniversary and looking to the next decade. ASR 36(3):320–326

Hugentobler U, Schaer S, Beutler G, Bock H, Dach R, Jäggi A, Meindl M, Urschl C, Mervart L, Rothacher M, Wild U, Wiget A, Brockmann E, Weber G, Habrich H, Boucher C (2003) In: Gowey K (ed) CODE IGS Analysis Center technical report 2002. IGS Central Bureau, Jet Propulsion Laboratory, Pasadena

Hugentobler, U, Dach R, Fridez P (2005) Bernese GPS software, version 5.0. Printing Office, University of Bern

Jäggi A, Hugentobler U, Beutler G (2004) Efficient stochastic orbit modeling techniques using least squares estimators. In: Sansó F (ed) A window on the future of geodesy. Springer, Berlin Heidelberg New York, pp 175–180

Jäggi A, Hugentobler U, Beutler G (2006) Pseudo-stochastic orbit modeling techniques for low Earth orbiters. J Geod 80(1):47–60

Press WH, Teukolsky A, Vetterling WT, Flannery BP (1996) Numerical recipes in Fortran 77—the art of scientific computing, 2nd edn. Cambridge University Press, Cambridge

Strang G, Borre K (1997) Linear algebra, geodesy, and GPS. Wellesley, Cambridge

Švehla D, Rothacher M (2002) Kinematic orbit determination of LEOs based on zero- or double-difference algorithms using simulated and real SST GPS data. In: Ádam J, Schwarz K-P (eds) Vistas for geodesy in the new millennium. Springer, Berlin Heidelberg New York

Švehla D, Rothacher M (2003) CHAMP double-difference kinematic POD with ambiguity resolution. In: Reigber C, Lühr H, Schwintzer P (eds) First CHAMP mission results for gravity, magnetic and atmospheric studies. Springer, Berlin Heidelberg New York

Teunissen PJG, Kleusberg A (eds) (1998) GPS for geodesy. Springer, Berlin Heidelberg New York

Visser PNAM, van den IJssel J (2003) Aiming at a 1-cm orbit for low Earth orbiters: reduced-dynamic and kinematic precise orbit determination. Space sciences series of ISSI. Earth gravity field from space—from sensors to Earth sciences. Kluwer, Dordrecht

Zumberge JF, Heflin MB, Jefferson DC, Watkins MM, Webb FH (1997) Precise point positioning for the efficient and robust analysis of GPS data from large networks. J Geophys Res 102(B3):5005–5017